Assessing Climate Impacts on West Nile Virus: An Interactive Vulnerability Map and a Preventative Policy Recommendation

Anaïs Teyton

June 2018

Acknowledgements

I would like to thank the members of my Capstone Advisory Committee for their time, support, and assistance throughout this process. I would like to especially express my gratitude to my advisor and Capstone Committee Chair, Tarik Benmarhnia, for his guidance and his assistance in making my aspiration of studying the nexus between climate and health possible. I am so appreciative for all of his help, from this Capstone to aiding me further my education after this program. I would also like to thank Morgan Levy for processing data used in this project, providing me with data resources, and helping me understand the ecological aspect of West Nile virus. I would like to thank Corey Gabriel for his advice and many discussions about the many facets of West Nile virus, particularly climate aspects, and I would like to thank Jason Vargo for his recommendations and expertise in data visualization.

I want to thank the people at the California Department of Public Health who provided monthly feedback and suggestions as well as presented me with resources to advance my Capstone, including Dorette English, Jason Vargo, and Robert Snyder.

I also extend many thanks to Joshuah Latimore, who designed the interactive map component of this Capstone, Rosana Aguilera Becker, who trained me in ArcGIS during the winter quarter, Amy Butros, who provided guidelines to using the UC San Diego library databases and referred me to pertinent UC San Diego resources, Amy Work, who furthered my knowledge of ArcGIS and taught me how to use web mapping interfaces, Mason McGhee, who guided me through Matlab coding, and Veronique Holley, who aided me in editing this paper.

Finally, I would like to thank the professors and students at Scripps Institution of Oceanography, UC San Diego, and San Diego State University for this remarkable year of learning.

Authorship

Anaïs Teyton
Master of Advanced Studies in Climate Science and Policy
Scripps Institution of Oceanography
University of California San Diego
ateyton@ucsd.edu | www.linkedin.com/in/anais-teyton

Capstone Advisory Committee

Tarik Benmarhnia, Ph.D | *Committee Chair & Expert Advisor*
Assistant Professor of Climate, Atmospheric Science, & Physical Oceanography and Family Medicine & Public Health
Scripps Institution of Oceanography and University of California San Diego

_____
Signature

Morgan Levy, Ph.D | *Committee Member*
Postdoctoral Researcher at the Global Policy and Strategy (GPS)
University of California San Diego

_____
Signature

Jason Vargo, Ph.D | *Committee Member*
Lead Research Scientist for the Climate Change and Health Equity Program
California Department of Public Health

_____
Signature

Corey Gabriel, Ph.D | *Committee Member*
Master of Advanced Studies Climate Science and Policy Executive Director
Scripps Institution of Oceanography

_____
Signature

Table of Contents

1. Abstract

West Nile virus is a vector-borne disease that is transmitted to humans from mosquitoes. It is the mosquito-borne disease that causes the most human cases in California. As humans burn fossil fuels, greenhouse gases are emitted. As anthropogenic greenhouse gas emissions cause climate change, California will experience warmer temperatures and infrequent but heavy rainfall (Pathak et al. 2018; Hayhoe et al. 2004). This climatic shift is ideal for mosquitoes, leading to increased mosquito abundance, more blood meals, faster virus replication rates and transmission, shortened incubation time between mosquitoes acquiring the infection and becoming infectious, and increased breeding sites (Paz 2015). These factors lead to facilitated transmission to humans and thus an increased risk in human outbreaks. As a result, it is important to observe past and present relationships between climate factors and West Nile virus human cases in order to prevent human cases in the future, where climate change impacts will become more severe. Many current California policies about preventative strategies against West Nile virus do not consider the influence

of climate change on West Nile virus. In order to be best prepared in future years, it seems necessary to include policy that recognizes West Nile virus prevention in the context of climate change.

An interactive vulnerability map was produced in order to observe which climate and socioeconomic factors contributed to West Nile virus human cases at the county-level in California. Climate factors, including average daily temperature (ºC), the number of days in a given week where the high temperature is 30ºC or below and the low is 14ºC or above, the weekly total of daily rainfall in millimeters, and the total number of rainy days in a given week in which rainfall exceeds 1 millimeter, were analyzed for relevant mosquito periods, which were the mosquito incubation period, the mosquito lifespan period, and the mosquito population growth period. Climate projection data, including maximum temperature and precipitation, from the Can-ESM2 climate model for RCP 8.5 was also collected up to the year 2100. Furthermore, socioeconomic factors, such as race and ethnicity, age, low birth weight, education linguistic isolation, poverty, and unemployment were observed to evaluate their association with human cases of West Nile virus. The census factors that are elevated in counties that also have high numbers of human cases include the Hispanic population percentage, the African American population percentage, the low birth weight percentage, the low education percentage, and the linguistic isolation percentage. This initiates an important discussion about unreported or under-reported cases of West Nile virus in California.

The interactive vulnerability map includes the selection of the type of factor as well as the year of interest by using drop-down menus. Moreover, an automated playthrough animation can be viewed for the selected variable. This map may be useful for the general public, policymakers, and researchers. The public can identify if they live in an at-risk county and implement preventative strategies if so. Policymakers can identify which groups of individuals are most at-risk of contracting West Nile virus, and they can support policies that involve co-benefits of climate change mitigation, including the reduction of vector-borne disease outbreaks in the future. Lastly, researchers may use this map in order to further their research projects as well as to include other vector-borne diseases to the map that are also affected by climate change.

Interactive tools, such as this vulnerability map, have the potential to aid California become better prepared for future vector-borne disease outbreaks as well as to further the discussion about the health benefits of mitigating climate change.

2. Introduction

2.1 From Uganda to California: The History of West Nile Virus & its Consequences

In 1937, the first reported case of West Nile virus was identified in the West Nile district of Uganda (Roehrig 2013). West Nile virus is a vector-borne disease, which means that it is transmitted by living organisms, specifically mosquitoes, that are infected by a virus (USGCRP 2016). It is caused by an arbovirus, which is a single-stranded RNA virus from the encephalitic *Flavivirus* genus ("West Nile Virus" 2017). For the following decades, West Nile virus caused small outbreaks throughout Africa and the Middle East (Bin et al. 2001). This included outbreaks in Egypt and Israel in the 1950's (Sejvar 2003). West Nile virus was subsequently spread by migratory birds to France in 1962 and South Africa in 1974 (Reiter 2010; Sejvar 2003). In 1994 and 1996, the virus caused outbreaks in Algeria and Romania, respectively, which were brought about by bird migration (Sambri et al. 2013). As West Nile virus was beginning to spread through Europe, the first North American case of West Nile virus occurred in New York in 1999. Though the mechanism by which the virus spread to the United States is unknown, possibilities include the movement of infected people, migratory birds, or the presence of infected mosquitoes on an aircraft or ship (Roehrig 2013; Rappole et al. 2000; Gyure 2009).

Within four years, West Nile virus augmented its geographic range from the East Coast to the West Coast (Sejvar 2003). In July of 2003, West Nile virus was first isolated in Imperial County, California from a pool of *Cx. Tarsalis* mosquitoes (W. Reisen et al. 2004). The mechanism by which the virus spread from the East coast to the West coast is also unknown; however, the timing of the California outbreak may provide insight as to which factors influenced this dispersal. First, the rise in West Nile virus transmission coincided with the timing of post-nesting movements by passerine bird species (W. Reisen et al. 2004). Second, within the month prior to the initial

outbreak, temperatures were above average and there were multiple rainfall events associated with the southwestern monsoon (W. Reisen et al. 2004). Counter-cyclonic flow around a strong, high pressure system over the state of Nevada enhanced the typical monsoonal flow, with particularly strong advection of moist air from the deep tropics into Southern California. These climate conditions are known to increase mosquito abundance. Third, it is possible that West Nile virus dispersed due to commerce via one of the East-West highways. A truck transporting goods may have enclosed infected mosquitoes, leading to their presence in California once they left the trucks (W. Reisen et al. 2004).

2.2 Medical Impacts of West Nile Virus

Since the virus's arrival in the United States, a total of 46,086 human cases were reported from 1999 to 2016 ("West Nile Virus" 2016). West Nile virus causes a range of effects on humans from an asymptomatic infection to severe symptoms, including encephalitis and meningitis. Approximately 80% of individuals who contract West Nile virus are asymptomatic, while almost 20% develop flu-like symptoms, such as fever, headache, body aches and pains, vomiting, diarrhea, or a rash ("West Nile Virus" 2017). Furthermore, about 0.67% of individuals who contract West Nile virus will develop very severe, neuroinvasive symptoms, including encephalitis, which is the inflammation of the brain, meningitis, which is the inflammation of the membranes that surround the brain and spinal cord, and acute flaccid paralysis, which is the onset of limb weakness (DeBiasi and Tyler 2006). These neuroinvasive symptoms occur following the viral penetration of the blood brain barrier; the neurons, especially those in the brainstem, deep nuclei, and anterior horn of the spinal cord, are directly invaded by the virus (DeBiasi and Tyler 2006). Specific groups of people are more susceptible to the viral penetration of the blood brain barrier and thus neuroinvasive symptoms of West Nile virus, including the elderly and immune-deficient individuals (Montgomery and Murray 2015). It has been shown that it takes most individuals with non-neuroinvasive West Nile virus approximately a year to fully recover (Loeb et al. 2008); however, it takes more time for neuroinvasive cases to make a full recovery to normal mental and physical conditions. In addition, individuals that had additional health issues at the time of West Nile virus onset were also found to take more time to recover (Loeb et al. 2008).

From census data collected from 2003 through 2016, a total of 3,389 cases of neuroinvasive West Nile virus were detected in California, and a total of 246 Californians have died directly due to this disease ("West Nile Virus" 2017). Thus, West Nile virus is one of the most impactful vector-borne diseases and the most severe mosquito-borne disease in California.

2.3 Ecological and Climate Factors Behind West Nile Virus Transmission

Specific factors, particularly ecological and climate factors, allow West Nile virus to propagate more effectively. Mosquito species, the primary vectors that transmit this virus, are capable of spreading the virus to other species, including humans, birds, horses, and other

mammals (Paz 2015). Birds and mosquitoes cyclically infect one another as mosquitoes bite infected birds and subsequently transmit the disease to the next bird they bite (Bernard et al. 2001). This viral amplification cycle often begins in the spring and ends in the fall (Petersen and Marfin 2002). Typically, if the environmental factors influencing West Nile virus, such as climate as well as host and vector presence, are ideal, an increased number of mosquitoes that also bite humans will be infected in summer (Petersen and Marfin 2002). This poses a larger risk of infection to humans in the late summer months. Both horses and humans are dead end hosts, which means that neither species is capable of transmitting this disease amongst its own species or other species, thus ending the transmission cycle (Colpitts et al. 2012). The transmission cycle of this virus is shown in Figure 1.

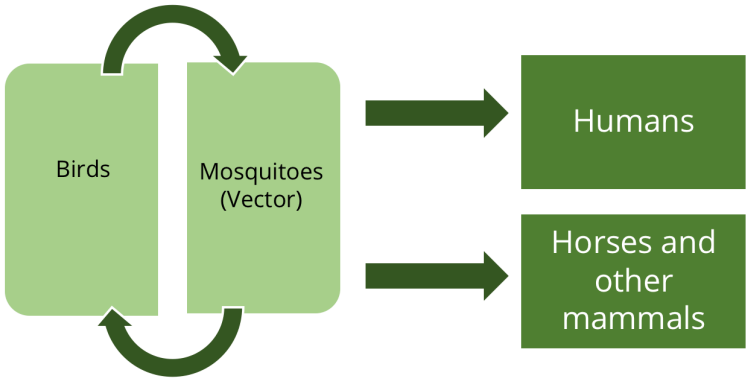

Figure 1: The West Nile virus transmission cycle ("California West Nile Virus Website" 2018).

Specific mosquito and bird species are more affected by West Nile virus than others. Within California, there are approximately ten known species of mosquito vectors that transmit West Nile virus, with its primary vector being the mosquito genus *Culex (Cx.)*; the mosquito genera *Ochlerotatus*, *Aedes*, and *Culiseta* transmit the virus as well, although to a lesser extent than the *Cx.* mosquitoes in California (Goddard et al. 2002). The *Cx. tarsalis* species is the dominant West Nile virus vector in rural agricultural systems, while *Cx. pipiens* compex species are the primary vector in urban areas (Goddard et al. 2002; Barker, Eldridge, and Reisen 2010). Moreover, West Nile virus especially impacts bird species within the Corvidae family (Wheeler et al. 2009). Birds with the highest risk of West Nile virus infection in California include the American Crow, the House Finch, the Black-crowned Night-Heron, the Western Scrub-Jay, and the Yellow-billed Magpie (Wheeler et al. 2009).

The relationship between bird and mosquito infection can be indicative of future human cases. Dead birds that are positively tested for West Nile are correlated with previously identified, positively tested mosquito samples (Mostashari et al. 2003). Furthermore, human infection and death due to West Nile virus are correlated to these previously detected dead birds. This makes

dead bird surveillance an effective early warning system for West Nile virus infections in humans (Guptill et al. 2003; Mostashari et al. 2003). Thus, it is critical to identify the timing of transmission among bird and mosquito species that leads to human infection.

There are three critical periods related to mosquitoes that occur prior to human cases that are important to observe in the context of human infection. In a human case of West Nile virus, the incubation period, which is the timing between the infection by mosquito and the clinical appearance of the illness, for that individual is approximately one week (Petersen and Marfin 2002). Prior to the time when the mosquito is capable of transmitting West Nile virus, the mosquito incubation period lasts approximately two weeks (W. K. Reisen, Fang, and Martinez 2005). The period in which the mosquito that will become infected is born and develops occurs four to twelve weeks prior to the human case. Finally, the period during which the mosquito population is breeding and growing occurs thirteen weeks before the human case and lasts one full year. During each of these periods, which are depicted in Figure 2 below, specific factors may contribute to ideal mosquito population growth, mosquito survival, and accelerating the mosquito incubation time. These factors may be indicative or an increased or decreased risk of human infections.

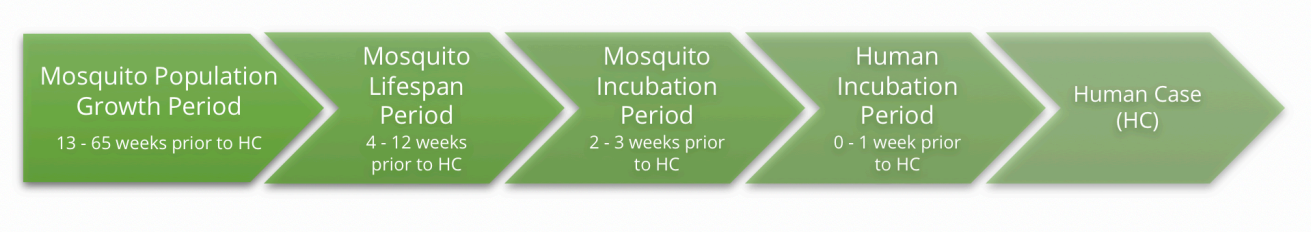

Figure 2: Timeline of relevant mosquito periods prior to human case.

West Nile virus is particularly affected by climate, and as climate change impacts are exacerbated over time, the risk of West Nile virus outbreaks may increase in specific regions. Climate factors can influence bird and mosquito dispersal, population, mosquito biting rates, incubation time, and survival rates as well as viral replication, amplification, and transmission (W. Reisen et al. 2004; Paz 2015). These climate factors include temperature, precipitation, humidity, wind, and changes in the seasonal cycle of temperature.

Temperature, a significant climate driver, impacts West Nile virus transmission (Crimmins et al. 2016). The temperature range for West Nile virus transmission from mosquitoes to humans is from 14-30 ºC (William K Reisen, Fang, and Martinez 2006). Increased temperatures may cause mosquito populations to grow, accelerate their life cycle, have more blood meals, increase the virus replication rate and virus transmission, and shorten the incubation time between acquiring the infection and becoming infectious in mosquito populations (Paz 2015; Crimmins et al. 2016). With the exception of high temperatures above the transmission threshold, the effects of

increased temperature on mosquito populations have shown an increased trend in human disease risk (Crimmins et al. 2016). Temperatures will increase over time due to climate change, and its influence of West Nile virus will consequentially have more profound effects (Paz 2015). These higher average temperatures may also lead to the northward expansion of West Nile virus (Harrigan et al. 2014).

Drought conditions, long dry periods with infrequent rainfall events, have led to increased West Nile virus outbreaks, as standing water attracts mosquitoes and birds and increases their proximity to one another (Paz 2015; Morin and Comrie 2013). In cases of flooding, mosquito populations may immediately decrease; however, over time, mosquito populations may rise and disease outbreaks in humans may increase (Paz 2015). Climate change due to human emissions has been shown to increase the likelihood of high-temperature, low-precipitation conditions in the western United States, which increases West Nile virus incidence (Diffenbaugh, Swain, and Touma 2015).

Neither relative humidity nor wind patterns are as robust of West Nile virus predictors as air temperature or precipitation; however the average maximum relative humidity is associated with vector population dynamics and morbidity in humans (Paz 2015). Furthermore, wind patterns may cause West Nile virus to spread by wind-blown mosquitoes, and bird migrations may shift (Paz 2015).

Mosquito populations are greatly affected by the seasonal cycle of temperature. As mentioned earlier, mosquitoes infect humans and other species in the late spring, summer, and early fall months. Beginning around the middle or end of October, female *Cx*. mosquitoes begin to overwinter, meaning they enter a dormant period, as the temperatures drop consistently to 10ºC or below (Nelms et al. 2013). The overwintering of these mosquitoes involves a developmental pause until the beginning of spring around the month of March, although the mosquitoes may continue to be infected with West Nile virus through the overwintering period (Nelms et al. 2013).

Climate change also has an effect on the seasonality of West Nile virus vectors. A decrease in abundance of mosquito populations and an increase in immature mortality during the hottest period in summer have been observed in arid habitats (Morin and Comrie 2013). When temperatures exceed the 14-30ºC temperature range, immature survival of mosquito larvae decreases (Ciota et al. 2014). Thus, a higher abundance of mosquitoes may be observed over the summer and beginning of fall as average temperatures increase due to climate change, though a decrease in mosquito abundance during the hottest peak of summer would occur. The highest abundance of mosquitoes would also shift later in the season than in current conditions, as optimal warm temperatures will occur later in the fall. The presence of mosquito populations extending into both the early spring and end of fall seasons has been witnessed due to increased temperatures as well as late summer and fall precipitation (Morin and Comrie 2013). If winters

become milder or shorter due to climate change, this will aid mosquitoes to survive and remain abundant, as it is difficult for them to survive longer, colder winters (Crimmins et al. 2016).

Climate change is already leading to shifts in these climatic factors, and it is possible that the transmission dynamics of West Nile virus will drastically change over time. Thus, it is important to study these effects in order to prevent further human cases of West Nile virus.

2.4 Capstone Project Motivation

Certain individuals are currently more vulnerable to contracting West Nile virus, and they will possibly be more severely affected in the future than the general public given climate change impacts. Generally, individuals who are most at-risk of West Nile virus infections are the elderly, individuals with compromised immune systems, individuals who spend time outdoors, and individuals who live in close proximity to stagnant water (Montgomery and Murray 2015). It is crucial to identify these populations and to locate which counties in California are more susceptible to West Nile virus.

The question posed and discussed by Dr. Marm Kilpatrick is one that is fundamentally important to answer, particularly for the state of California:

> Are the worst West Nile virus epidemics… behind us? West Nile virus epidemics peaked in many states the year after it arrived with fewer human cases having been observed subsequently. This reduction in West Nile virus disease has led to reduced research focus and less funding from public health agencies for West Nile virus, and more recently, less testing for West Nile virus by health care providers… If West Nile virus transmission is regulated by climate, then severe epidemics could recur, especially if they are facilitated by climate change (Kilpatrick 2011).

It is critical to investigate the effects of climate on West Nile virus in the state of California. Unlike other states, West Nile virus did not peak the year after it was identified in California; rather, it seems as though a large outbreak has occurred every two to three years after the first case of West Nile virus in 2003. This is shown in Figure 1. It is possible that climate change may intensify these larger outbreaks, as the effects of climate change have been seen as favorable to increase the abundance of mosquitoes and thus the increased risk of transmission to humans.

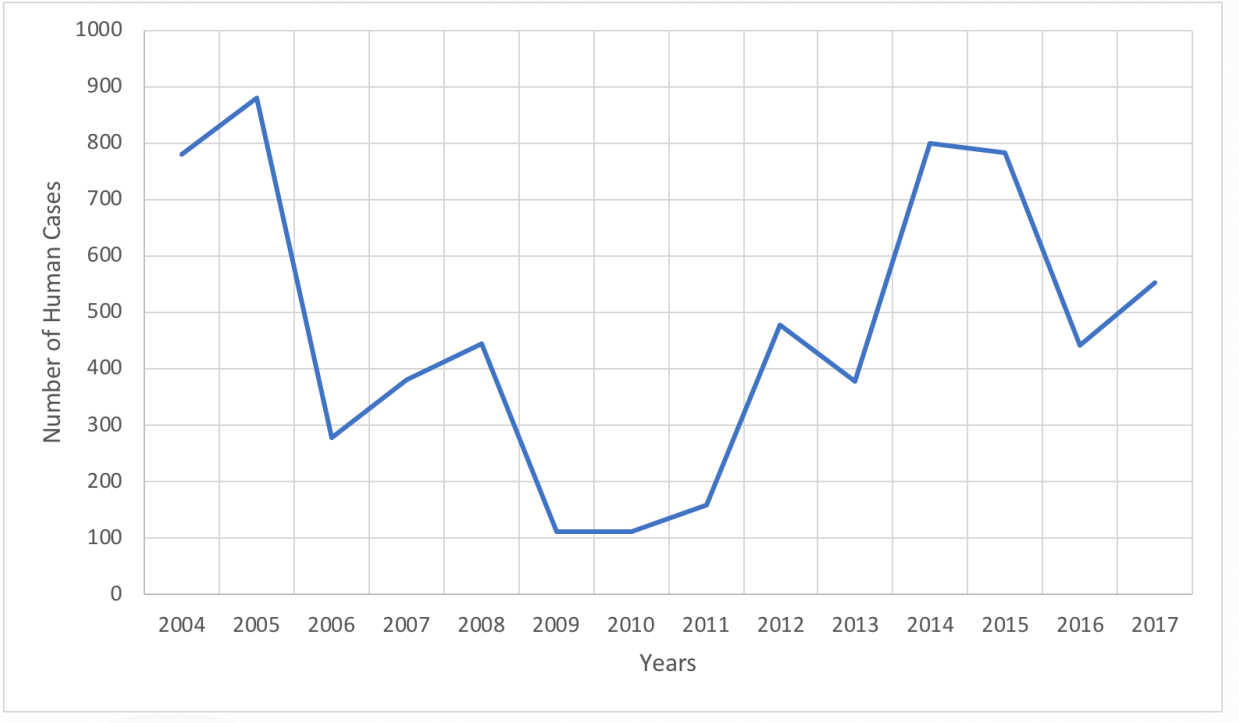

Figure 3: Reported Cases of West Nile Virus in California from 2003 to 2017 ("California West Nile Virus Website" 2018).

The effects of a changing climate must be studied in order to answer the following questions: Are climate factors affecting this outbreak cycle? Which counties in California are most affected by the relationship between climate and West Nile virus? Will these outbreaks be exacerbated in the future?

This project involves the creation of an interactive vulnerability map in order to summarize the role of key climate features in determining West Nile virus risk at the county-level in California. West Nile virus, climate, and census data were assessed in order to discern vulnerable populations. These data were analyzed to identify which factors have the most significant impact on human cases presently and in the future, and those impacts were visually represented in an interactive map interface. By identifying key climate features that put people at risk of contracting West Nile virus, and identifying which areas are at most risk, policies may be suggested and then implemented in order to best prevent further cases of the disease.

Although scientific experts warn of the impact climate change may have on West Nile virus, especially in the future, many prevention policies in California do not consider or strategize about how to minimize this imminent threat from climate change. In order to be fully prepared for future dangers, California policies should include measures about how to prepare and prevent future outbreaks in the face of climate change. Given the possibility of increased human risk with

the warming of temperature and increased prospect of drought with climate change in future years, this map has the possibility of instigating awareness amongst individuals, such as the general public, policymakers, and researchers, about vulnerable populations and at-risk counties in California as well as the importance of mitigating climate change in order to decrease the threat of vector-borne disease outbreaks in the future.

3. Data and Methods

First, a literature review was conducted in order to better understand West Nile virus transmission, the relationship between West Nile virus vectors and climate factors, and the impacts of West Nile virus on human populations in California. Publicly-available weekly data on human cases of West Nile virus, sentinel chickens testing positive for West Nile virus, mosquito samples testing positive for West Nile virus, and dead birds testing positive for West Nile virus from years 2006 to 2017 were collected from the California Department of Public Health West Nile Virus website ("California West Nile Virus Website" 2018). From these data, initial maps were created for each of these variables (i.e., human cases, sentinel chickens, etc.) for the specified range of years. This allowed for better visualization of which counties have had the most reported infections and which years caused the most impact.

Publicly-available daily weather data from the Parameter-elevation Regressions on Independent Slope Models (PRISM) Climate Group at Oregon State University's website were processed and used as well ("Prism Climate Group" 2018). This daily, county-level data was aggregated into weekly county-level summary statistics in order to match the West Nile virus data. The following summary climate statistics (hereafter, "climate factors) were used: Average daily temperature (ºC), the number of days in a given week where the high temperature is 30ºC or below and the low is 14ºC or above, the weekly total of daily rainfall in millimeters, and the total number of rainy days in a given week in which rainfall exceeds 1 millimeter. Weather data processing was carried out using the statistical software, R (R Core Team 2014). These climate factors were chosen in order to conduct an exploratory analysis to observe which factors were most likely to influence the risk of West Nile virus human infections.

These four climate factors were analyzed during the mosquito incubation period, the mosquito lifespan period, and the mosquito population growth period (Figure 1). These periods were defined as occurring prior to the week with the maximum number of human cases within a given county for a specified year. Based on relevant literature (see Introduction), the mosquito incubation period occurs on average 2 to 3 weeks prior to the week with the maximum human cases, the mosquito lifespan period occurs on average 4 to 12 weeks prior to the week with the maximum human cases, and the mosquito population growth period on-average occurs 13 to 65 weeks prior to the maximum human cases, which is a total of a one-year period. These three

mosquito periods were identified for each of the 58 counties for the years 2006 to 2017. The average, the maximum, the minimum, and the standard deviation of these four climate factors during each of the three mosquito periods were calculated for individual counties from 2006 to 2017. These 48 climate factors were mapped for each year within the range. These climate factors were also averaged over the 12-year period (see Appendix for Figures 12-23). While the climate factors for each individual year are not included in this report, the climate factors averaged over the 12-year period are included; these averaged climate factor maps were used as diagnostic plots to guide the final analysis and to observe which factors were associated with increased human cases.

Publicly-available census data was also collected from the 2014 California Communities Environmental Health Screening Tool, which is made available by the Office of Environmental Health Hazard Assessment (OEHHA). The following socioeconomic factors at the county-level were collected: Race and ethnicity percentages, age percentage (percent of the population under the age of 10 and over the age of 65), low birth weight percentage, education percentage (percent of the population over 25 with less than a high school education), linguistic isolation percentage (percent of households in which no one 14 and over speaks English "very well" or speaks English only), poverty percentage (percent of the population that is living below two times the federal poverty level), and unemployed percentage (percent of the population over the age of 16 that is unemployed and eligible for the labor force). These census factors were selected in order to explore which social and economic factors may be able to determine increased West Nile virus human cases.

After the data collection process, a principal component analysis (PCA), a multivariate data analysis technique, was used to simplify the high-dimensional data, which included both climate and socioeconomic data (Wold, Esbensen, and Geladi 1987). A PCA jointly simplifies complex data into fewer dimensions while retaining crucial trends and information from the data (Lever, Krzywinski, and Altman 2017). By using a PCA, contrasting climate and census factors can be compared to one another. Variables called principal components are computed by the PCA, which are then used as the axes upon which the data will be projected (Abdi and Williams 2010). The principal components maximize the variance within the data, where the first principal component (PC1) is indicative of the direction with the most variation of the data (Abdi and Williams 2010). The subsequent principal components represent the direction of the next most variation in the data and must be orthogonal to its previous component (Abdi and Williams 2010). PC1 was selected as the PC to analyze, as it best describes the data and its variation. The influence of each climate and census factor on PC1 can be scored as an eigenvector value, which was found using the data analysis carried out using the statistical software, STATA (StataCorp 2017). When the factor's score is large in either the positive or negative direction, then the factor has a large influence on the PC1 and is significant. If the score is close or equal to zero, then the factor has

minimal influence on PC1 and is insignificant. [Explain why the analysis is useful; ex: in summary, factors contributing substantial variation in West Nile virus case incidence can be identified in this way]

Three vulnerability indexes were built based on the PC1 eigenvector values as well as the corresponding climate and census factors. These indexes allowed for counties to be directly compared to each other based on the vulnerability indexes and factors. The three vulnerability indexes were found by calculating the total sum of the products of each factor's PC1 eigenvector value and the value of the factor averaged over the 12-year period for each county. First, the "climate index" was calculated based on the maximum and standard deviation of the four climate factors for each of the three relevant mosquito periods. Second, a "census index" was calculated based on the all of the selected census factors. Third, a "climate and census index" was calculated based on both the maximum and standard deviation of the four climate factors for each of the three relevant mosquito periods as well as the selected census factors. and census. It is important to note that these indexes highlight factors with principal component scores that are large in either the positive or negative direction. These indexes were mapped as well.

Projection data from the Cal-Adapt website were used in order to observe changes in temperature and precipitation at the county-level in the future ("LOCA Downscaled Climate Projections" 2018). Annual averages of maximum temperature and average precipitation from 2006 to 2099 for each county were downloaded. One future scenario was used for these climate projections, which was RCP 8.5. RCP 8.5 includes a future where both population growth and greenhouse gas emissions continue to increase, where radiative forcing will increase to 8.5 Watts per meter squared by the year 2100 (Hayhoe et al. 2017; van Vuuren et al. 2011). This scenario can be seen in Figure 4 below. By observing shifts in temperature and precipitation using this extreme-case RCP scenario, a climate change signal that affects West Nile virus may be identified.

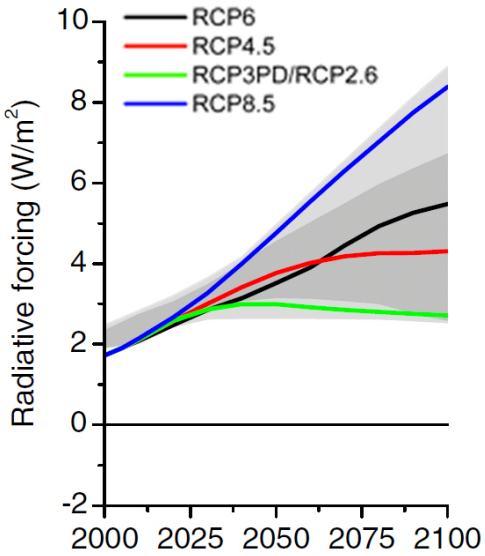

Figure 4: Representative Concentration Pathways (RCP) scenarios from years 2000 to 2100. RCP 8.5 is represented in blue. Figure retrieved from ("Scenario Process for AR5," n.d.).

From this data, an interactive map was assembled. The objective for the interactive component of the vulnerability map was for different groups of individuals, such as the general public, policymakers, and researchers, to be able to easily use to map, to be able to compare different factors amongst each other, and to make meaningful connections with this map. Aspects of various available interactive maps were examined, such as the "Yale Climate Opinion Maps" as well as those presented in articles including the New York Time's "A Peek Into Netflix Queues" and Bloomberg's "Climate Change Dilemma for Coastal America: How Much Flooding is Too Much?" (Howe et al. 2015; Bloch et al. 2010; Flavelle and Levitt 2017). Outlines for this interactive vulnerability map were map and compared using tools including informational popups, a sliding bar for years, selected factor filter, various drop-down menus, and animated demonstrations of change in selected factor over time. Preferred color bins for legends that would aid in visualizing differences within and between the surveillance, climate, census, and index datasets and that would be visible to individuals who are colorblind were chosen by using the Color Brewer website (Brewer et al. 2013).

4. Results

4.1 Descriptive Maps

A map of California with labeled counties is included in the Appendix (Figure 5). From 2006 to 2017, the counties with the highest total number of human cases were Los Angeles,

Orange, and Kern (Figure 6). Los Angeles county had a significantly higher than average number of human cases for the years 2008, 2009, 2011, 2012, 2013, 2015, and 2016. Orange county had a significantly higher than average number of human cases for 2008 as well as 2014. Kern county had a significantly higher than average number of human cases for years 2006, 2007, 2009, and 2010. The counties that are typically higher with respect to human cases are located in Southern California, with the exception of Imperial county, and the southern Central Valley around Fresno. The exception to this trend occurred in 2006, where Butte and Yolo counties in Northern California were higher than average. Human cases were lower in most of Northern California and Eastern California counties.

The highest human case years within the 2006-2017 period, in decreasing order, include 2014, 2015, and 2017 (Figure 11). The counties that had the highest maximum number of human cases within the span of a week over the 2006-2017 period include Los Angeles and Orange. Above-average counties with a high maximum number of human cases include most counties in Southern California and the Central Valley, while Northern and Eastern California counties have lower-than-average maximum number of human cases. Within the 2006-2017 period, the years with the highest human fatalities, in decreasing order, were 2015, 2017, and 2014 ("California West Nile Virus Website" 2018).

The counties with the highest total count of dead birds include Sacramento, Los Angeles, and Santa Clara (Figure 7). Sacramento county had a significantly higher than average number of dead bird cases for the years 2007, 2011, and 2012. The years in which Los Angeles had a higher than average number of dead bird cases include 2007, 2009, 2011, and 2012. Santa Clara had a significantly higher than average number of dead bird cases for 2006, 2014, and 2015. The counties that are typically higher with respect to dead bird cases are located in Southern California, with the exception of Imperial county, and the counties surrounding Sacramento county. Counties that are lower than average include Northern and Eastern California, along with the central coastline counties. The highest dead bird case years within the 2006-2017 period, in decreasing order, include 2008, 2014, and 2012.

The counties with the highest total count of mosquito samples include Los Angeles, Sacramento, and Kern (Figure 8). Los Angeles had a significantly higher than average number of mosquito samples for the years 2008, 2011, 2013, 2014, 2016, and 2017. The years in which Sacramento had a higher than average number of mosquito samples include 2007, 2008, 2010, 2011, 2013, 2014, and 2016. Kern had a significantly higher than average number of mosquito samples for 2006, 2007, 2009, 2010, and 2011. The counties that are higher with respect to mosquito samples are located in the northern region of Southern California, including Kern, Riverside, and Los Angeles, the southern region of the Central Valley, including Tulare and Fresno, and the Sacramento region. The highest mosquito sample years within the 2006-2017 period, in decreasing order, include 2016, 2017, and 2015.

The counties with the highest total count of positive sentinel chickens within the period of 2006-2017 include Los Angeles, Kern, and Riverside (Figure 9). Los Angeles had a significantly higher than average number of positive sentinel chickens for the years 2008, 2011, 2012, 2013, and 2015. Kern had a significantly higher than average number of positive sentinel chickens for the years 2006, 2010, 2011, and 2012. The years in which Riverside had a higher than average number of mosquito samples include 2008 and 2010. The counties that have higher counts of positive sentinel chickens include Butte county and its surrounding counties, Tulare county and its surrounding counties, and Southern California counties, including Kern, Los Angeles, San Bernardino, and Riverside. In comparison, counties in Northern and Eastern California, the northern Central Valley, and the entire Californian coastline excluding Los Angeles have lower than average counts of positive sentinel chickens. The highest positive sentinel chicken years within the 2006-2017 period, in decreasing order, include 2006, 2008, and 2012.

The counties with the highest average incidence proportion of human cases within the period of 2006-2017 include Glenn, Butte, and Colusa (Figure 10). Glenn had a significantly higher than average incidence proportion for the years 2006, 2008, 2010, 2012, 2013, 2015, and 2016. Butte had a significantly higher than average incidence proportion for the year of 2008. Colusa had a significantly higher than average incidence proportion for 2008 and 2012. The counties that have a higher incidence proportion include Butte and its surrounding counties as well as Fresno and its surrounding counties. In contrast, the counties along a majority of the California coastline, Northern and Eastern California, and the Southern counties of San Diego and Imperial had lower than average incidence proportions. The highest incidence proportion years, in decreasing order, include 2006, 2015, and 2014.

4.2 Climate Maps

The weekly average temperature in Celsius, the count of favorable temperature days, the precipitation sum in millimeters, and the count of days where precipitation is greater than 1 millimeter were calculated for each of the three periods. The mean, maximum, minimum, and standard deviation were found for these four variables. The maps of these variables averaged over 2006 to 2017 for the three mosquito periods are included in the Appendix. Counties without human cases are colored white as “no data.”

The maps of the mosquito period mean, maximum, minimum, and standard deviation of weekly average temperature were very similar amongst the incubation, lifetime, and population growth periods (Figures 12, 16, and 20 for incubation period, lifetime period, and population growth periods, respectively). The main difference among these all-year maps are the Northern counties, including Siskiyou and Modoc counties, which are above average for the standard deviation maps but below average for the mean, maximum, and minimum maps. Most of the above-average counties reside in Southern California, including San Bernardino, Riverside, Imperial, and Inyo counties, and certain counties in the Butte county region. In contrast, some of

the below average counties include the Central California coastline as well as some of the Northern counties.

The maps of the mosquito period mean, maximum, minimum, and standard deviation of favorable temperature count were also similar amongst the incubation, lifetime, and population growth periods (Figures 13, 17, and 21 for incubation period, lifetime period, and population growth periods, respectively). There were two significant differences between the maps: Both Alameda and Orange counties are above average for the minimum favorable temperature count for the incubation and lifetime periods, while the population growth period does not include any above-average counties for the minimum favorable temperature count. Furthermore, the incubation period maps also have more below-average counties, such as Imperial county and more counties along the Western coast while San Francisco county was above average. Most counties in Southern California as well as Placer, Nevada, Alameda, and Santa Clara counties are above average for favorable temperature count, while some Northern, Eastern, and Western coastal counties were below average.

The maps of the mosquito period mean, maximum, minimum, and standard deviation of precipitation sum contrasted among the different mosquito periods (Figures 14, 18, and 22 for incubation period, lifetime period, and population growth periods, respectively). Within the mean, maximum, and standard deviation precipitation sum maps for the incubation period, the three above-average counties included San Francisco, Santa Clara, and Amador. Meanwhile, Santa Barbara and Solano counties were above average for the minimum of precipitation sum during the incubation period. During the lifetime period, Santa Cruz and Amador counties remained above average for the mean, maximum, and standard deviation of precipitation sum, while Northern counties showed higher precipitation sums and Southern counties had lower precipitation sums. Modoc and Siskiyou counties were above average for the minimum of precipitation sum for the lifespan period. For the mean, maximum, and standard deviation of precipitation sum maps for the population growth period, the Southern counties were below-average, while Northern counties, such as Butte, were above-average.

The maps of the mosquito period mean, maximum, minimum, and standard deviation of precipitation count also contrasted among the different mosquito periods (Figures 15, 19, and 23 for incubation period, lifetime period, and population growth periods, respectively). A clear trend in county regions cannot be identified for either the incubation period or the lifespan period, although some of the Southern counties, such as Inyo, were higher than average, while many Northern counties were either close to the average or below average; the Amador county area region was overall above-average. In contrast, the maps for the precipitation count for the population growth period resembled the maps for the precipitation count for the lifespan period; Southern counties are significantly below-average, while northern counties are significantly above-average. This indicates that in the population growth period, Northern counties have more

precipitation days and a larger precipitation sum, while Southern counties have less precipitation days and a smaller precipitation sum.

Overall, it seems that there is a positive correlation between temperature factors and human cases and a negative correlation between rainfall factors and human cases. The favorable temperature count maps show this positive correlation with human cases more so than the average temperature maps do. Similarly, the rainfall day count maps show this negative correlation with human cases more so than the precipitation sum maps do. The climate factors in both the lifespan period and the population growth period also seem to be more indicative of human cases than climate factors in the incubation period.

4.3 Census and Index Maps

Census factor maps are shown in Figures 24, 25, and 26, while the index map is shown in Figure 27. The census factor maps that most resemble the human case maps include the Hispanic population percentage, the African American population percentage, the low birth weight percentage, the low education percentage, and the linguistic isolation percentage. The poverty percentage and the unemployment percentage include some similarities with the human case map, particularly the above-average counts in the Fresno county area. The average number of individuals within the county population is very similar to the human case maps. In comparison, the climate factor maps that resemble the human case maps the least include the white population percentage, Native American population percentage, the Asian American percentage, the other ethnicity population percentage, and the age above 65 and below 10 population percentage.

The index maps are shown in Figure 27. The census index map resembles the human case maps, while the climate index as well as the climate and census index maps do not resemble the human case maps at all. The census index is higher than average for Los Angeles, Orange, San Diego counties. Both the climate index as well as the climate and census index are below-average in Southern California counties, and they do not have significantly higher than average counties. It seems as though the climate components, particularly the precipitation factors, have a larger impact on the climate and census index than the census components. The precipitation factors had a larger influence on the climate index, as the climate index map has many similarities to the precipitation sum and precipitation sum maps; the Southern counties are lower than average while the Northern counties are higher than average.

4.4 Projection Maps

The climate projection maps from the CanESM2 model using RCP 8.5 can be seen in Figures 28, 29, and 30. The rate of change over the time period 2006 to 2100 were calculated for both maximum temperature as well as precipitation.

The counties of Orange, Ventura, Santa Barbara, Kern, San Luis Obispo, and Tulare were the counties with the slowest rates of change for maximum temperature from 2006 to 2100. In contrast, the counties of Trinity, Siskiyou, Modoc, and Lassen were the counties with the fastest rates of change for maximum temperature over this time period. There is a clear distinction between Northern and Southern California, where Northern California counties have faster rates of change for maximum temperature, while Southern California counties have slower rates of change.

The only county that has a significantly slower rate of change for precipitation is Imperial county, while the counties with significantly higher rates of change for maximum temperature were Sonoma, Santa Cruz, Sierra, Nevada, Alpine, and Tuolomne.

The annual maximum temperature projection over the years shows that there is an overall warming across all of California. With RCP 8.5, counties such as Imperial, Riverside, and San Bernardino will exceed the ideal mosquito temperature range of 14-30ºC, while northern counties will remain within the upper boundary of the ideal temperature range. There is a noticeable gradient, where maximum temperature increases in the southward direction. In comparison, the northern counties have heavier precipitation over time than southern counties. There is an overall increase in precipitation within most counties across California. There is also a noticeable gradient, where precipitation decreases in the southward direction.

4.5 Interactive Vulnerability Map

The components of the interactive vulnerability map are depicted in Figures 31, 32, and 33. The data type may be selected by using a drop-down menu, which includes surveillance or climate factor by year, climate projection by year, average climate projection data, index data, and census data. From this selection, the data variable may then be chosen from a drop-down menu, which includes the specific surveillance factors, climate factors associated with mosquito periods, climate projection factors, climate projection factors averaged over the decades from 2020 to 2100, the three indexes, and the census factors. When applicable, the year for the chosen data variable may be selected, and an automated playthrough animation of the time period can be selected for the chosen variable. Furthermore, a desired county may be clicked on, which allows for a pop-up to appear with a plot of the selected data variable over the relevant time period for that county.

5. Discussion

5.1 Interpretation of Results

It is clear from the maps that the counties with high human cases are most likely related to high dead bird, mosquito samples, and sentinel chicken counts. The incubation period climate factors were not indicative of human cases; however, the climate factors in the lifespan and

population growth periods are more indicative of human cases. During the lifespan period, counties with increased temperature count also have increased human cases, while counties with lower precipitation sum also have increased human cases. This relationship is more apparent amongst the temperature count and precipitation sum factors; however, a positive relationship can be observed between human cases and average temperature, while a negative relationship can be observed between human cases and precipitation count. These relationships become more evident in the population growth period. These associations were further justified using Poisson regression models, which showed the negative association between human cases and precipitation and the positive association between human cases and temperature.

The Hispanic population percentage, the African American population percentage, the low birth weight percentage, the low education percentage, and the linguistic isolation percentage were the census factors that are positively associated with human cases. The relationships between human cases and races are particularly interesting, as a majority of individuals who are reported with West Nile virus diseases cases are white. From 1999 to 2008, out of 11,288 United States patients with available race data, 95% of patients were white (Lindsey et al. 2010). This calls into question the number of cases that go unreported, and if specific groups of individuals are more vulnerable to remain unreported than others. It is possible that specific groups may be under-reported due to factors including linguistic barriers, poverty, or not having the knowledge that they should go to the hospital when having specific symptoms. This was seen in a study which compared the effects of West Nile virus on Hispanic agricultural workers in Kern and Coachella Valley. Coachella Valley is closer to Mexico, and it is possible that Hispanic agricultural workers who are uninsured may travel to Mexico, as the cost to treat is lower there than within the United States. This study recognized an ethnic segregation between individuals who may seek treatment and be tested by physicians and those who may not seek this aid due to the cost or may not be tested by physicians (W K Reisen et al. 2009). These groups may be less under-reported if doctors are trained to test for West Nile virus if associated symptoms are present.

The census index as well as the census and climate index were shown to not be adequate indicators to identify counties with a higher risk of human cases. It seems that precipitation factors had a significant influence when performing the Principal Component Analysis in both the climate index as well as the climate and census index. This may be the reason why Southern counties in these maps have below-average index values, while Northern counties have above-average index values. The census index was a more robust indicator of increased West Nile virus risk in comparison to both the climate index as well as the census and climate index. The census index had above-average index values in Southern counties that also had increased human cases; in addition, the census index also had below-average index values in Northern counties that also had minimal human cases.

The climate projections show an increase in both maximum temperature and precipitation over time, with higher maximum temperatures in Southern California and higher precipitation in Northern California. It is important to acknowledge that RCP 8.5 was used for these projections, which is considered the highest emissions pathway. Using RCP 8.5 and the Can-ESM2 model, by 2100, much of the Southern California and parts of Central California would exceed the maximum temperature threshold for ideal mosquito survivability and West Nile virus transmission. Northern counties become warmer as well, and their maximum temperature shifts to the upper bounds of the ideal mosquito temperature range. Thus, it a northward shift of West Nile virus may be possible in the future, and a northward movement in North America has been observed in the past two decades (Paz 2015).

5.2 Preventative and Adaptation Policy Measures

In order to prevent further cases of West Nile virus that may be exacerbated by climate change as well as to prepare the public for a potential increased risk of disease, policy measures must be implemented. Surveillance methods are currently in place in order to isolate and identify West Nile virus in non-human species within specific areas before they infect humans. These surveillance methods affect the decision of whether or not more serious measures should be implemented in order to eradicate West Nile virus, including techniques to control mosquito populations. Educating the public on how to best prepare against West Nile virus through a variety of means can lead to a reduction of disease cases. It is important to compare the costs and benefits of each of these preventative and adaptive policy measures to the consequences of West Nile virus cases that are left unmanaged.

5.2.1 Surveillance Methods

There are several surveillance methods in place in California, including mosquito vectors, avian hosts, and sentinel chickens (Healy et al. 2014). Equine and human infection testing were also used as surveillance methods, although these are no longer considered sensitive indicators of vector activity (Brown 2017). Equine infections are not used as a sensitive indicator because horses, donkeys, and mules become more immune to the virus over time than other species (Brown 2017). Furthermore, human infections are also unused as a sensitive indicator, as so many individuals who are infected are asymptomatic or require a few weeks before the symptoms become apparent (Brown 2017); thus, they are not exemplary indicators that could be used to plan and implement emergency control plans.

Both mosquito abundance as well as mosquito infections can be used as surveillance methods. These methods are measured by collecting mosquito samples from high mosquito density pools, and these collection sites are registered by county level agencies on the California Vectorborne Disease Surveillance System (CalSurv) website (Smith and Brown 2018). Both samples of immature and adult mosquitoes are collected for this measure. Mosquito infections can also aid in detecting virus activity, where adult mosquitoes are tested for West Nile virus (E. Brown 2017). Mosquito infections are tested for in the early season, including spring and early

summer, and it has been shown to be one of the most efficient methods to detect West Nile virus (Brown 2017; Healy et al. 2014). Both of these measures, mosquito abundance and infections in mosquitoes, have been used as inputs in prospective models that forecast future human cases, which was done for the state of South Dakota (Davis et al. 2017). Furthermore, the estimated weekly cost for mosquito traps is approximately $72 per week (Healy et al. 2014).

Dead birds can be collected and tested for West Nile virus. The California Department of Public Health has encouraged the public to submit reports online regarding where and when they have seen dead or sick birds as a means to detect West Nile virus ("California West Nile Virus Website" 2007). These dead birds are then tested to see if they died from the virus (E. Brown, 2017). The estimated weekly cost for collecting and testing dead birds is approximately $65 per week (Healy et al. 2014). A specific limitation to dead bird sampling is that it is unknown whether or not the birds died from the virus itself or from other causes. Furthermore, selection bias is present when testing these birds, as they are not all equally detected and reported by the general public.

Finally, state and local agencies collaborate in order to place flocks of chickens in locations where mosquito density is known to be high or where virus activity has been recently present (E. Brown, 2017). The sites used for these sentinel chickens are also registered by county level agencies on the CalSurv website (Smith and Brown 2018). These previously unexposed chicken flocks of 6-10 chickens are tested every two weeks by the California Department of Public Health for West Nile virus (E. Brown 2017). If chicken seroconversion is present, then the chicken has developed antibodies in order to fight off the virus. The estimated weekly cost for chicken flocks is approximately $111 per week, which is the most expensive of the three surveillance methods (Healy et al. 2014).

It is necessary to have surveillance methods in place in order to prevent widespread transmission to humans. The efficiency and cost of the three major West Nile virus surveillance methods, which are mosquito samples, dead bird testing, and sentinel chicken flocks, have been analyzed. The mosquito trappings and publicly-reported dead birds were reported to detect West Nile virus earlier than the serological monitoring of sentinel chickens by two and five weeks, respectively (Healy et al. 2014). Publicly-reported dead birds were found to be the most cost-effective surveillance method of the three (Healy et al. 2014). Sentinel chickens detected more positive West Nile virus results in the later season, while mosquitoes detected more positive West Nile virus results in the early season (Healy et al. 2014). Sentinel chicken flocks could be reduced from flocks of ten to flocks of six or seven without reducing surveillance sensitivity (Healy et al. 2014). The most cost-effective surveillance monitoring would be to use a combination of these three methods: Mosquito testing in the early season, reduced sentinel chicken flocks in the late season, and dead bird detections used throughout the entire season (Healy et al. 2014).

When these surveillance methods detect increased virus activity, mosquito control methods are often implemented.

5.2.2 Controlling Mosquito Larvae and Adult Populations

When mosquitoes are known to be infected with West Nile virus in specific areas, various methods to control the mosquito populations may be implemented. Mosquito control is proven to be the only method that can currently protect populations from West Nile virus (E. Brown 2017). These methods are implemented by mosquito control agencies as well as county health departments (E. Brown, 2017). Two specific types of mosquito control methods can be implemented, which are larval control and adult control.

Mosquito larval control methods are the more utilized option, as larvae are densely concentrated in aquatic habitats and more easily reduced ("Best Management Practices for Mosquito Control in California" 2012; Brown 2017). Larval control uses environmental management, biological control, and chemical control in order to reduce larvae (E. Brown, 2017). Environmental management involves multiple factors. Source elimination removes possible mosquito habitats in urbanized areas, which includes eliminating pools of stagnant water, filling ditches that could hold stagnant water with sediments, and covering structures or containers that could hold water ("Best Management Practices…" 2012). Both source reduction and maintenance attempt to eliminate the time that water is left standing in ecosystems, which include reducing vegetation growth in wetlands, digging ditches in order to maintain water circulation, creating drainage ditches to limit flooding, and removing debris from stormwater channels ("Best Management Practices…" 2012). Biological controls involve the use of predators, parasites, and pathogens to limit the abundance of mosquito larvae (Brown 2017). The most frequently used biological control by local mosquito control agencies is the mosquitofish, which are highly effective at consuming mosquito larvae in areas such as ponds and wetlands ("Best Management Practices…" 2012). Certain microbes have been used as well as surface films, although these have been shown to have negative effects on other aquatic insect species (E. Brown 2017). Finally, larvicides may be implemented, which include bio-rational products, surface films, insect growth regulators, and chemical products, all of which must be approved by the California Department of Public Health for use ("Best Management Practices…" 2012). Bio-rational products use natural toxins that are found in certain bacteria, surface films use mineral oils or alcohol-derived films on the water surface to prevent larvae from breathing, insect growth regulators affect the physiological development of larvae, and chemical pesticides can be used to control larvae populations, although they are rarely implemented ("Best Management Practices…" 2012).

Adult mosquito controls are implemented when larvae control is not possible or when immediate action on the reduction of mosquito populations must be done (E. Brown 2017). Adult controls are made up of ultralow volumes of chemicals including organophosphates, pyrethroids, and pyrethrins, which are applied on the ground or by aircraft (E. Brown 2017). These pesticides cost millions of dollars in California; for reference, $9.4 million were spent to purchase pesticides between 2005 and 2007, which does not include the cost of applying these pesticides on the

ground or by aircraft (Howard et al. 2010). Though negative effects from these adulticides are rare, individuals should limit their exposure to these ultralow volume applications by staying indoors while they are being conducted ("Best Management Practices…" 2012). The schedule for adulticide application is provided online by county level vector control agencies ("Best Management Practices…" 2012).

The final component for preventative policy measures is public education, which can reduce the abundance of mosquitoes as well as reduce potential human cases through specific practices.

5.2.3 Public Education and Outreach

Educating the public about personal protection against West Nile virus as well as techniques to reduce mosquito abundance around their homes and areas where they work contribute to a decrease in human disease cases and reduce mosquito populations.

Individuals are taught to minimize standing water, as this is where mosquitoes lay eggs and larvae develop. The general public can learn to discard containers that can store standing water, such as tires, buckets, and cans, empty unused pools, and unclog rain gutters (E. Brown 2017). Farmers can be taught about effective irrigation practices that limit standing water, while wetland managers and rangers can work with local mosquito control agencies to limit flooding and allow for proper water circulation (E. Brown 2017).

Furthermore, the public can be educated to change certain habits or to develop new habits in order to limit their exposure to infected mosquitoes. Mosquito repellents containing DEET can be used and can be taught how to correctly wear (Schwarzenegger, Belshé, and Horton 2008). These repellents should be used over clothing, not underneath clothing, and they should be used sparingly on direct skin contact (Schwarzenegger, Belshé, and Horton 2008). Repellents that have ingredients such as lemon eucalyptus oil and picaridin can also be used, although these repellents must be applied more often than those containing DEET (Schwarzenegger, Belshé, and Horton 2008).

Individuals who spend time outdoors can learn to limit their outdoor time when mosquito biting levels are high, which are predominantly during the hours of dusk as well as dawn (E. Brown 2017). Long-sleeved clothing can also be worn outdoors as this may reduce the possibility of being bitten by infected mosquitoes (E. Brown 2017). Individuals can also repair screens, windows, and doors in their houses to prevent mosquitoes from coming inside their homes ("West Nile Virus" 2017). Furthermore, physicians and veterinarians can learn to be observant for West Nile virus symptoms and to request lab tests as a means to enhance clinical surveillance (E. Brown 2017).

The predominant method of outreach for public awareness is through the California Department of Public Health's West Nile virus website as well as county level public health and vector control program websites. The statewide "Fight the Bite!" campaign also increases public awareness through billboards, its website, fliers on the West Nile virus at ranger stations and

trailheads, and child-friendly games ("California West Nile Virus Website" 2018). Most individuals are aware of West Nile virus, but many do not exercise protective behaviors (Fox et al. 2006). It seems that more rigorous campaigns may be used in the future in order to make individuals aware of the severity of West Nile virus and to make individuals exercise the protective behaviors mentioned above (Fox et al. 2006). This mapping tool is a promising means to communicate to the public through an interactive and engaging way.

5.3 Comparison to Related Mapping Tools & Next Steps

Quite a few interactive maps involving climate and health exist for air pollution and extreme heat; however, fewer exist for vector-borne diseases in the context of climate change. The Natural Resources Defense Council website includes a "Infectious Disease Vulnerability 1995-2005" tab for human cases of Dengue fever at the state-level in the United States (Knowlton 2015). The Companion Vector-Borne Diseases website includes a world map with a variety of vector-borne diseases, including which vectors and comments are relevant to the selected region ("Occurrence Maps" 2017). West Nile virus is not included in this Companion Vector-Borne Diseases map. The California Survey Research Services includes California maps of a few vector-borne diseases, including West Nile virus, for the locations of mosquito pools, sentinel chickens, and dead birds ("California Surveillance Gateway Maps" 2018). The exact dates can be selected from 2003 to 2018, which leads to these factors being projected onto the map. The Centers for Disease Control and Prevention includes a map of the United States at the county-level for many vector-borne diseases, including West Nile virus, including human, mosquito, bird, sentinel animal, and veterinary cases from years 2003 to 2017 ("ArboNET Disease Maps" 2018).

A minimal number of states acknowledge climate factors that can impacts the transmission of West Nile virus. The Arizona Department of Health Services conducted two reports that include climate impacts and projections of West Nile virus as well as a vulnerability assessment in the Southwestern United States, such as the states of Arizona, California, Colorado, Nevada, New Mexico, and Utah (Roach, Brown, Clark, et al. 2017; Roach, Brown, Wilder, et al. 2017). Other states do not include reports as thorough as Arizona's; Texas is the only state that expresses that a key limitation in its West Nile virus guide was the lack of climate data analysis in the context of the virus ("West Nile Virus Public Health Preparedness, Surveillance, and Response Guide" 2015).

Some of the next steps for this interactive map include the addition of relevant bird periods as well as the inclusion of other social determinants. Bird periods, including breeding, lifetime, and virus infection and incubation, occur at different times than the relevant mosquito periods. It may be interesting to include the climate factors that occurred during these bird periods prior to human cases in order to identify whether or not these factors may be indicative of future human cases. Furthermore, additional sociodemographic determinants may be studied in order to identify their correlation with human cases of West Nile virus. This may include identifying the relationship between factors such as population density, homeless population

percentage, medically-underserved population percentage, and land use classification with West Nile virus infections. It will be crucial to identify underreported populations; if physicians can learn to include West Nile virus as a possibility when patients come in with relevant symptoms, then these populations can be correctly identified. These populations can then be educated on how to prevent future infections. Furthermore, mosquito species that are present within California counties can be identified to see which species more effectively infect humans. By including these factors, a more wholesome map of West Nile virus and its relationship with climate and social determinants may be assembled. This map may help supplement public outreach efforts and provide a range of data that can be used to further investigate how West Nile virus transmission may shift.

6. Conclusion

The implementation and integration of public health policies that address the influence of climate change will be necessary in order to prevent future possible West Nile virus outbreaks in California. West Nile virus epidemics peaked in multiple states after the initial outbreak in the United States, and there has been a small number of human cases in those states since (Kilpatrick 2011). Because of this trend, less funding on West Nile virus from public health agencies has been available, which has led to a decreased research focus on the disease and less clinical testing in hospitals (Kilpatrick 2011). California has witnessed multiple, severe outbreaks since 2003, particularly in the years 2005, 2014, and 2015. Climate change will bring increased average temperatures and shifts in precipitation, which have the potential to increase the risk of future West Nile virus outbreaks. It is important to be prepared for possible future outbreaks by conducting further research investigations on these influential climatic factors and by implementing policies that protect vulnerable populations.

This interactive vulnerability map will allow the public, policymakers, and researchers to understand crucial aspects of West Nile virus. The public can identify whether or not they live in an at-risk county, learn more about the virus as well as the effects of climate change on the virus, and apply preventative strategies in order to minimize their risk of infection. Policymakers can understand the gravity of the virus, realize the need to identify groups of individuals who are underreported with the disease, and advocate for the co-benefits of climate change mitigation policies that will limit the impact of vector-borne diseases. Researchers may also use this map in order to further their own research projects and to include other vector-borne diseases that are impacted by climate factors.

Tools must be created to measure the impact of climate change on vector-borne diseases, as these may reduce detrimental health effects. Mitigating climate change means protecting the health of all populations, including those at risk of diseases such as West Nile virus. The emerging shift in attention on climate and health has the potential to instigate widespread social change if

effectively communicated to the public. By actualizing climate and health work that can be meaningful to a range of individuals like this interactive map, California will be better prepared for future human cases and West Nile virus epidemics, more capable of reducing the future risk of infection, and more effective at communicating the importance of mitigating climate change.

7. References

Abdi, Hervé, and Lynne J. Williams. 2010. "Principal Component Analysis." *Wiley Interdisciplinary Reviews: Computational Statistics*. https://doi.org/10.1002/wics.101.

"ArboNET Disease Maps." 2018. Centers for Disease Control and Prevention. 2018. https://wwwn.cdc.gov/arbonet/maps/ADB_Diseases_Map/index.html.

Barker, Christopher M, Bruce F Eldridge, and William K Reisen. 2010. "Seasonal Abundance of Culex Tarsalis and Culex Pipiens Complex Mosquitoes (Diptera: Culicidae) in California." *Journal of Medical Entomology* 47 (5):759–68. https://doi.org/10.1603/ME09139.

Bernard, K. a., J. G. Maffei, S. a. Jones, E. B. Kauffman, G. Ebel, a. P. Dupuis, K. a. Ngo, et al. 2001. "West Nile Virus Infection in Birds and Mosquitoes, New York State, 2000." *Emerging Infectious Diseases* 7 (4):679–85. https://doi.org/10.3201/eid0704.010415.

"Best Management Practices for Mosquito Control in California." 2012.

Bin, H, Z Grossman, S Pokamunski, M Malkinson, L Weiss, P Duvdevani, C Banet, et al. 2001. "West Nile Fever in Israel 1999-2000 from Geese to Humans." *Ann N Y Acad Sci* 951 (1):127–42. https://doi.org/10.1111/j.1749-6632.2001.tb02691.x.

Bloch, Matthew, Amanda Cox, Jo Craven McGinty, and Kevin Quealy. 2010. "A Peek Into Netflix Queues." The New York Times. 2010.

Brewer, Cynthia, Mark Harrower, Ben Sheesley, Andy Woodruff, and David Heyman. 2013. "ColorBrewer." The Pennsylvania State University. 2013.

Brown, Edmund. 2017. "California Mosquito-Borne Virus Surveillance & Response Plan."

"California Surveillance Gateway Maps." 2018. California Survey Research Services. 2018. https://maps.calsurv.org/.

"California West Nile Virus Website." 2007. 2007.

———. 2018. 2018. http://www.westnile.ca.gov/.

Ciota, Alexander T, Amy C Matacchiero, A Marm Kilpatrick, and Laura D Kramer. 2014. "The Effect of Temperature on Life History Traits of Culex Mosquitoes." *Journal of Medical Entomology* 51 (1):55–62. https://doi.org/10.1603/ME13003.

Colpitts, Tonya M., Michael J. Conway, Ruth R. Montgomery, and Erol Fikrig. 2012. "West Nile Virus: Biology, Transmission, and Human Infection." *Clinical Microbiology Reviews* 25 (4):635–48. https://doi.org/10.1128/CMR.00045-12.

Crimmins, A, J Balbus, J L Gamble, C B Beard, J E Bell, D Dodgen, R J Eisen, et al. 2016. "Human Health the Impacts of Climate Change on in the United States the Impacts of Climate Change on Human Health in the United States." *U.S. Global Change Research Program*, 25–42. https://doi.org/10.7930/J0GQ6VP6.

Davis, Justin K., Geoffrey Vincent, Michael B. Hildreth, Lon Kightlinger, Christopher Carlson, and Michael C. Wimberly. 2017. "Integrating Environmental Monitoring and Mosquito Surveillance to Predict Vector-Borne Disease: Prospective Forecasts of a West Nile Virus Outbreak." *PLoS Currents*, 1–23. https://doi.org/10.1371/currents.outbreaks.90e80717c4e67e1a830f17feeaaf85de.

DeBiasi, Roberta L., and Kenneth L. Tyler. 2006. "West Nile Virus Meningoencephalitis." *Nature Clinical Practice Neurology*. https://doi.org/10.1038/ncpneuro0176.

Diffenbaugh, Noah S., Daniel L. Swain, and Danielle Touma. 2015. "Anthropogenic Warming Has Increased Drought Risk in California." *Proceedings of the National Academy of Sciences* 112 (13):3931–36. https://doi.org/10.1073/pnas.1422385112.

Flavelle, Christopher, and Daniel Levitt. 2017. "Climate Change Dilemma for Coastal America: How Much Flooding Is Too Much?" *Bloomberg*, July 12, 2017.

Fox, Michael H., Ellen Averett, Gail Hansen, and John S. Neuberger. 2006. "The Effect of Health Communications on a Statewide West Nile Virus Public Health Education Campaign." *American Journal of Health Behavior* 30 (5):483–94. https://doi.org/10.5993/AJHB.30.5.5.

Goddard, Laura B., Amy E. Roth, William K. Reisen, and Thomas W. Scott. 2002. "Vector Competence of California Mosquitoes for West Nile Virus." *Emerging Infectious Diseases* 8 (12):1385–91. https://doi.org/10.3201/eid0812.020536.

Guptill, Stephen C., Kathleen G. Julian, Grant L. Campbell, Susan D. Price, and Anthony A. Marfin. 2003. "Early-Season Avian Deaths from West Nile Virus as Warnings of Human Infection." *Emerging Infectious Diseases* 9 (4):483–84. https://doi.org/10.3201/eid0904.020421.

Gyure, Kymberly A. 2009. "West Nile Virus Infections." *Journal of Neuropathology and Experimental Neurology*. https://doi.org/10.1097/NEN.0b013e3181b88114.

Harrigan, Ryan J., Henri A. Thomassen, Wolfgang Buermann, and Thomas B. Smith. 2014. "A Continental Risk Assessment of West Nile Virus under Climate Change." *Global Change Biology* 20 (8):2417–25. https://doi.org/10.1111/gcb.12534.

Hayhoe, K., D. Cayan, C. B. Field, P. C. Frumhoff, E. P. Maurer, N. L. Miller, S. C. Moser, et al. 2004. "Emissions Pathways, Climate Change, and Impacts on California." *Proceedings of the National Academy of Sciences* 101 (34):12422–27. https://doi.org/10.1073/pnas.0404500101.

Hayhoe, K., J. Edmonds, R.E. Kopp, A.N. LeGrande, B.M. Sanderson, M.F. Wehner, D.J. Wuebbles, et al. 2017. "Climate Models, Scenarios, and Projections." *Climate Science Special Report: Fourth National Climate Assessment* I:133–60. https://doi.org/10.7930/J0WH2N54.

Healy, J M, W K Reisen, V L Kramer, M Fischer, N Lindsey, R S Nasci, P A Macedo, et al. 2014. "Comparison of the Efficiency and Costs of West Nile Virus Surveillance Methods in California." *American Journal of Tropical Medicine and Hygiene* 91 (2):254. https://doi.org/10.1089/vbz.2014.1689.

Howard, Timothy S, Mark G Novak, Vicki L Kramer, and Larry R Bronson. 2010. "Public Health Pesticide Use in California: A Comparative Summary." *Journal of the American Mosquito Control Association* 26 (3):349–53. https://doi.org/10.2987/10-5997.1.

Howe, Peter D., Matto Mildenberger, Jennifer R. Marlon, and Anthony Leiserowitz. 2015. "Geographic Variation in Opinions on Climate Change at State and Local Scales in the USA."

Nature Climate Change 5 (6):596–603. https://doi.org/10.1038/nclimate2583.
Kilpatrick, A. Marm. 2011. "Globalization, Land Use, and the Invasion of West Nile Virus." *Science*. https://doi.org/10.1126/science.1201010.
Knowlton, Kim. 2015. "Climate Change Threatens Health." Natural Resources Defense Council. 2015.
Lever, Jake, Martin Krzywinski, and Naomi Altman. 2017. "Points of Significance: Principal Component Analysis." *Nature Methods*. https://doi.org/10.1038/nmeth.4346.
Lindsey, Nicole P, J Erin Staples, Jennifer A Lehman, and Marc Fischer. 2010. "Surveillance for Human West Nile Virus Disease - United States, 1999-2008." *Morbidity and Mortality Weekly Report. Surveillance Summaries (Washington, D.C. : 2002)* 59 (2):1–17. http://www.ncbi.nlm.nih.gov/pubmed/20360671.
"LOCA Downscaled Climate Projections." 2018. Cal-Adapt. 2018. http://cal-adapt.org/data/loca/).
Loeb, Mark, Steven Hanna, Lindsay Nicolle, John Eyles, Susan Elliott, Michel Rathbone, Michael Drebot, Binod Neupane, Margaret Fearon, and James Mahony. 2008. "Prognosis after West Nile Virus Infection." *Annals of Internal Medicine* 149 (4):232–41.
Montgomery, Ruth R., and Kristy O. Murray. 2015. "Risk Factors for West Nile Virus Infection and Disease in Populations and Individuals." *Expert Review of Anti-Infective Therapy* 13 (3):317–25. https://doi.org/10.1586/14787210.2015.1007043.
Morin, C. W., and A. C. Comrie. 2013. "Regional and Seasonal Response of a West Nile Virus Vector to Climate Change." *Proceedings of the National Academy of Sciences* 110 (39):15620–25. https://doi.org/10.1073/pnas.1307135110.
Mostashari, Farzad, Martin Kulldorff, Jessica J. Hartman, James R. Miller, and Varuni Kulasekera. 2003. "Dead Bird Clusters as an Early Warning System for West Nile Virus Activity." *Emerging Infectious Diseases* 9 (6):641–46. https://doi.org/10.3201/eid0906.020794.
Nelms, Brittany M, Paula A Macedo, Linda Kothera, Harry M Savage, and William K Reisen. 2013. "Overwintering Biology of Culex (Diptera: Culicidae) Mosquitoes in the Sacramento Valley of California." *Journal of Medical Entomology* 50 (4):773–90. https://doi.org/10.1055/s-0029-1237430.Imprinting.
"Occurrence Maps." 2017. The Companion Vector-Borne Diseases. 2017. http://www.cvbd.org/en/occurrence-maps/world-map/.
Pathak, Tapan, Mahesh Maskey, Jeffery Dahlberg, Faith Kearns, Khaled Bali, and Daniele Zaccaria. 2018. "Climate Change Trends and Impacts on California Agriculture: A Detailed Review." *Agronomy* 8 (25).
Paz, S. 2015. "Climate Change Impacts on West Nile Virus Transmission in a Global Context." *Philosophical Transactions of the Royal Society B: Biological Sciences* 370 (1665):20130561–20130561. https://doi.org/10.1098/rstb.2013.0561.
Petersen, Lyle R., and Anthony A. Marfin. 2002. "West Nile Virus: A Primer for the Clinician." *Annals of Internal Medicine*. https://doi.org/10.7326/0003-4819-137-3-200208060-00009.
"Prism Climate Group." 2018. Northwest Alliance for Computational Science and Engineering. 2018. http://www.prism.oregonstate.edu/.
Rappole, J. H., S. R. Derrickson, Z. Hubálek, and Z. Hubálek. 2000. "Migratory Birds and Spread of West Nile Virus in the Western Hemisphere." *Emerging Infectious Diseases* 6 (4):319–28. https://doi.org/10.3201/eid0604.000401.

Reisen, W. K., Y. Fang, and V. M. Martinez. 2005. “Avian Host and Mosquito (Diptera: Culicidae) Vector Competence Determine the Efficiency of West Nile and St. Louis Encephalitis Virus Transmission.” *Journal of Medical Entomology* 42 (3):367–75. https://doi.org/10.1603/0022-2585(2005)042[0367:AHAMDC]2.0.CO;2.

Reisen, W K, B D Carroll, R Takahashi, Y Fang, S Garcia, V M Martinez, and R Quiring. 2009. “Repeated West Nile Virus Epidemic Transmission in Kern County, California, 2004-2007.” *J Med Entomol* 46 (1):139–57. https://doi.org/10.1603/033.046.0118.

Reisen, William K, Ying Fang, and Vincent M Martinez. 2006. “Effects of Temperature on the Transmission of West Nile Virus by Culex Tarsalis (Diptera: Culicidae).” *Journal of Medical Entomology* 43 (2):309–17. https://doi.org/10.1603/0022-2585(2006)043[0309:eotott]2.0.co;2.

Reisen, William, Hugh Lothrop, Robert Chiles, Minoo Madon, Cynthia Cossen, Leslie Woods, Stan Husted, Vicki Kramer, and John Edman. 2004. “West Nile Virus in California.” *Emerging Infectious Diseases* 10 (8):1369–78. https://doi.org/10.3201/eid1008.040077.

Reiter, P. 2010. “West Nile Virus in Europe: Understanding the Present to Gauge the Future.” *Eurosurveillance*. https://doi.org/19508 [pii].

Roach, Matthew, Heidi E. Brown, Robert Clark, David Hondula, Joceline Lega, Quyymun Rabby, Nick Schweers, and Joseph Tabor. 2017. “Projections of Climate Impacts on Vector-Borne Diseases and Valley Fever in Arizona.”

Roach, Matthew, Heidi E. Brown, Margaret Wilder, Garrett Smith, Samuel Chambers, Iris Patten, and Quyymun Rabby. 2017. “Assessment of Climate and Health Impacts on Vector-Borne Diseases and Valley Fever in Arizona.”

Roehrig, John T. 2013. “West Nile Virus in the United States - A Historical Perspective.” *Viruses* 5 (12):3088–3108. https://doi.org/10.3390/v5123088.

Sambri, V, M Capobianchi, R Charrel, M Fyodorova, P Gaibani, E Gould, M Niedrig, et al. 2013. “West Nile Virus in Europe: Emergence, Epidemiology, Diagnosis, Treatment, and Prevention.” *Clinical Microbiology and Infection : The Official Publication of the European Society of Clinical Microbiology and Infectious Diseases* 19 (8):699–704. https://doi.org/10.1111/1469-0691.12211.

“Scenario Process for AR5.” n.d. Intergovernmental Panel on Climate Change.

Schwarzenegger, Arnold, Kimberly Belshé, and Mark Horton. 2008. “Best Management Practices for Mosquito Control on California State Properties.”

Sejvar, James J. 2003. “West Nile Virus: An Historical Overview.” *The Ochsner Journal* 5 (3):6–10. http://www.ncbi.nlm.nih.gov/pubmed/21765761%5Cnhttp://www.pubmedcentral.nih.gov/articlerender.fcgi?artid=PMC3111838.

Smith, Karen, and Edmund Brown. 2018. “Participating Agencies in the 2018 California Arbovirus Surveillance Program.”

StataCorp. 2017. “Stata Statistical Software: Release 15.” StataCrop LLC. 2017.

Team, R Core. 2014. “R: A Language and Environment for Statistical Computing.” R Foundation for Statistical Computing. 2014. http://www.r-project.org/.

USGCRP. 2016. “The Impacts of Climate Change on Human Health in the United States: A Scientific Assessment.” *Global Change Research Program*. https://doi.org/http://dx.doi.org/10.7930/J0R49NQX.

Vuuren, Detlef P. van, Jae Edmonds, Mikiko Kainuma, Keywan Riahi, Allison Thomson, Kathy Hibbard, George C. Hurtt, et al. 2011. “The Representative Concentration Pathways: An Overview.” *Climatic Change* 109 (1):5–31. https://doi.org/10.1007/s10584-011-0148-z.

“West Nile Virus.” 2016. Centers for Disease Control and Prevention. 2016. Final Cumulative Maps & Data for 1999-2016.

———. 2017. Centers for Disease Control and Prevention. 2017.

“West Nile Virus Public Health Preparedness, Surveillance, and Response Guide.” 2015.

Wheeler, Sarah S., Christopher M. Barker, Ying Fang, M. Veronica Armijos, Brian D. Carroll, Stan Husted, Wesley O. Johnson, and William K. Reisen. 2009. “Differential Impact of West Nile Virus on California Birds.” *The Condor* 111 (1):1–20. https://doi.org/10.1525/cond.2009.080013.

Wold, Svante, Kim Esbensen, and Paul Geladi. 1987. “Principal Component Analysis.” *Chemometrics and Intelligent Laboratory Systems* 2 (1–3):37–52. https://doi.org/10.1016/0169-7439(87)80084-9.

8. Appendices

Note:

The color legend for the descriptive, climate, census, index, and projection maps are as follows:

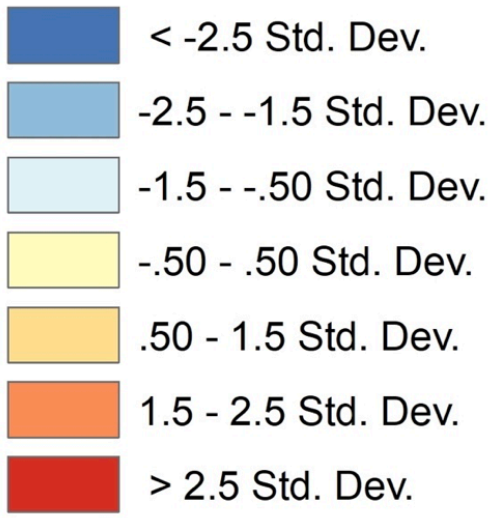

8.1 Descriptive Maps

Figure 5: Map of California labeled by county (made in ArcMap).

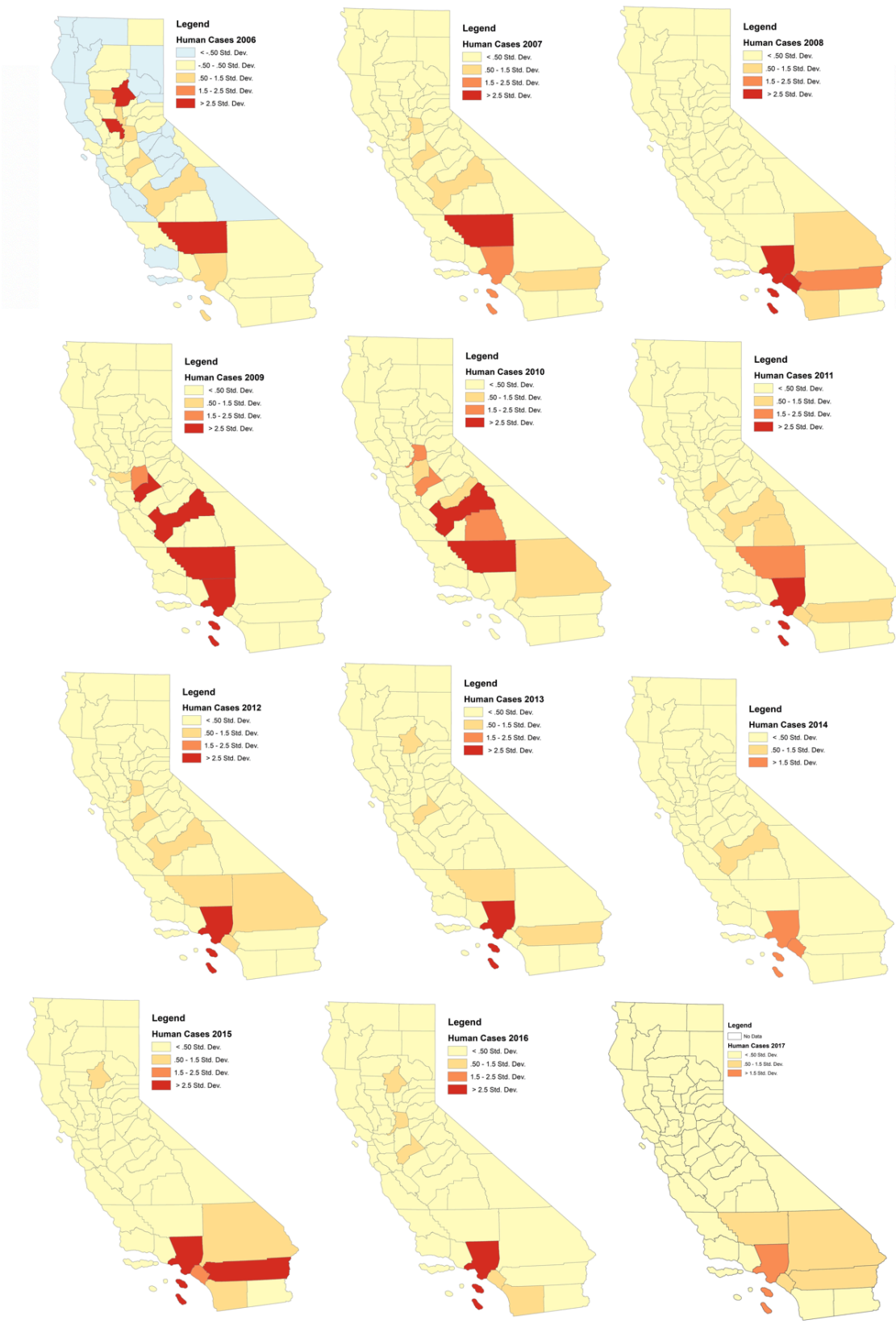

Figure 6: Number of human cases for years 2006-2009 (upper row), 2010-2013 (middle row), 2014-2017 (lower row) with color bins based on standard deviations away from the mean. Maps made in ArcMap.

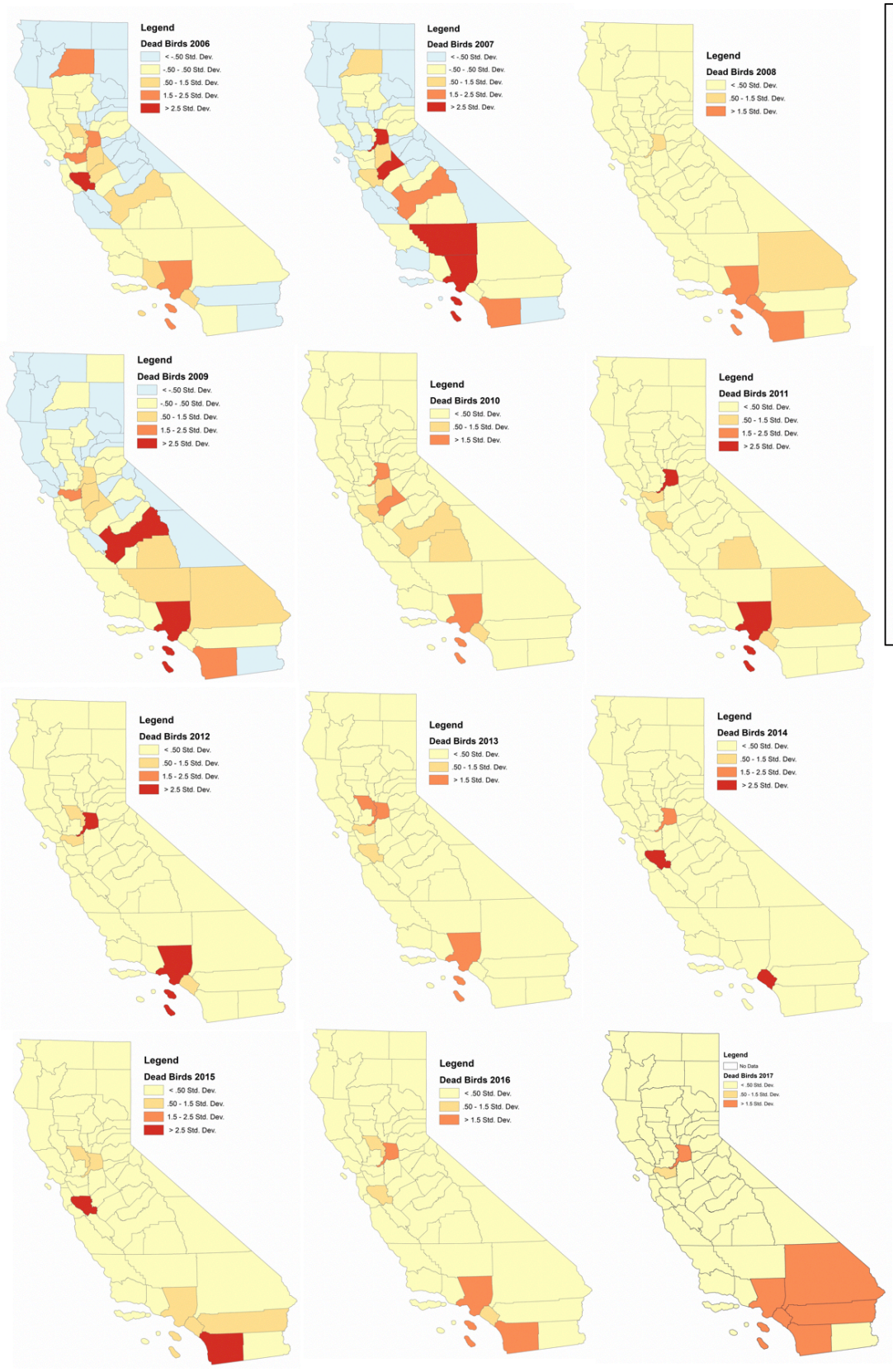

Figure 7: Number of dead bird cases for years 2006-2009 (upper row), 2010-2013 (middle row), 2014-2017 (lower row) with color bins based on standard deviations away from the mean. Maps made in ArcMap.

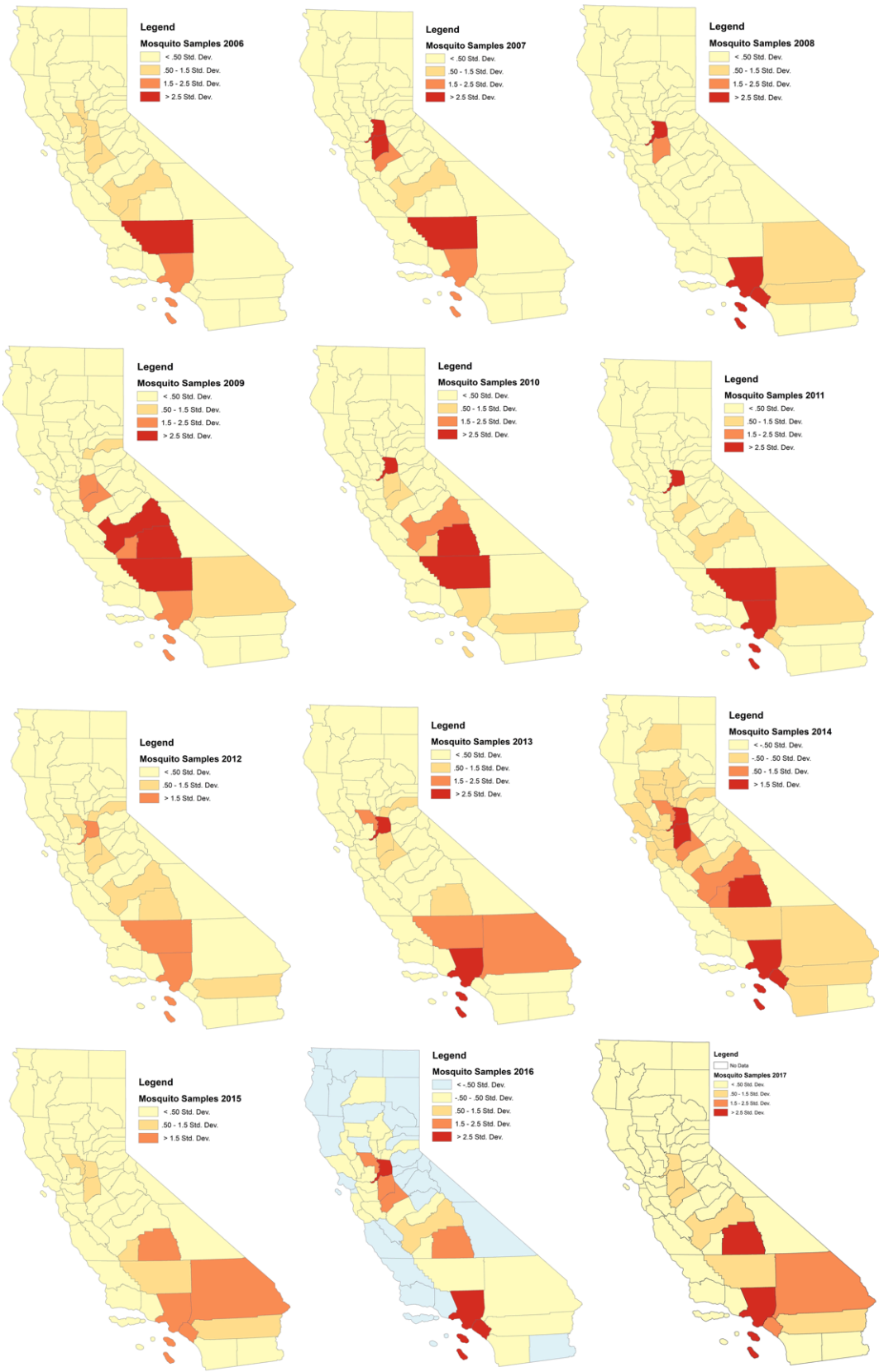

Figure 8: Number of mosquito sample cases for years 2006-2009 (upper row), 2010-2013 (middle row), 2014-2017 (lower row) with color bins based on standard deviations away from the mean. Maps made in ArcMap.

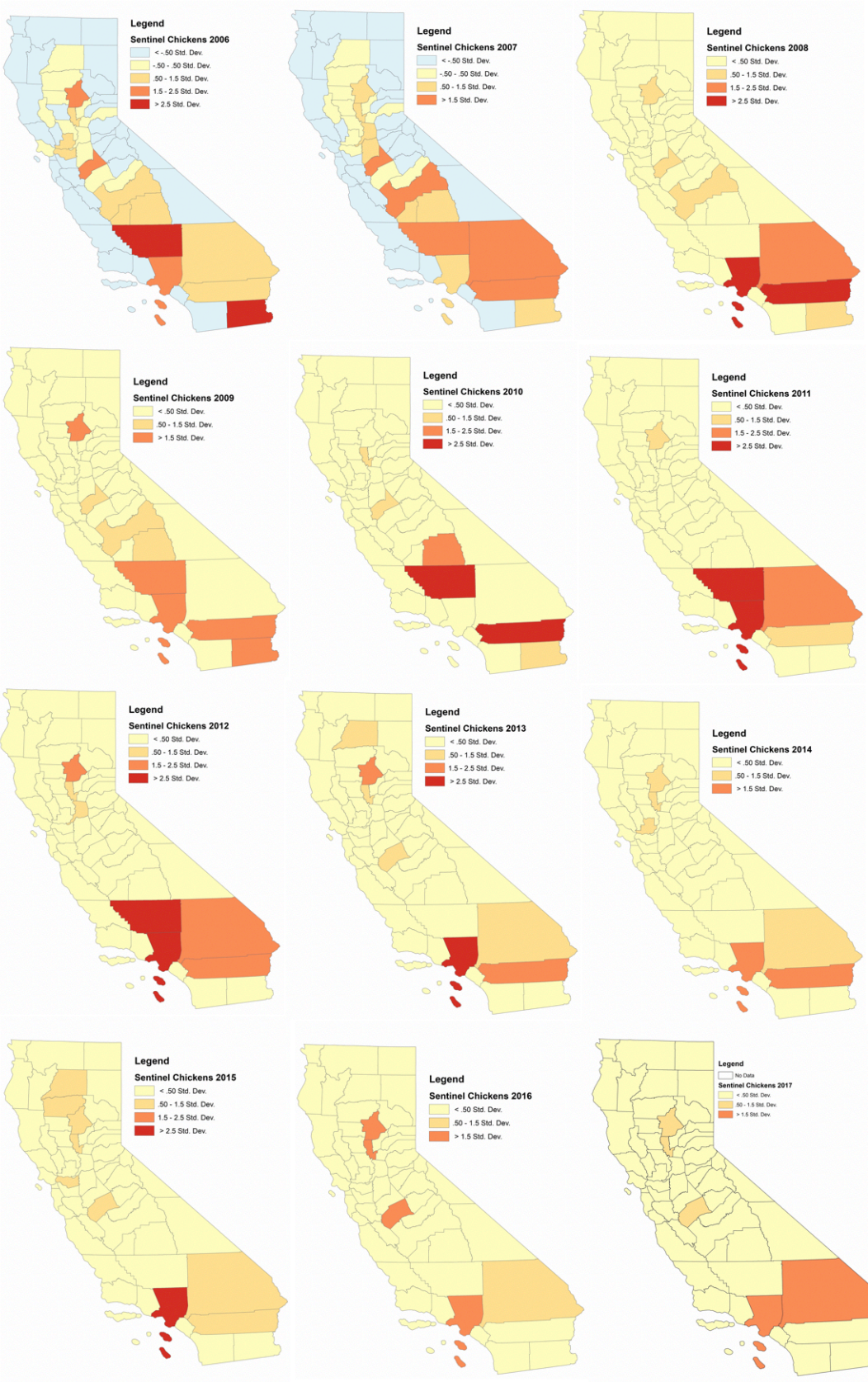

Figure 9: Number of sentinel chicken cases for years 2006-2009 (upper row), 2010-2013 (middle row), 2014-2017 (lower row) with color bins based on standard deviations away from the mean. Maps made in ArcMap.

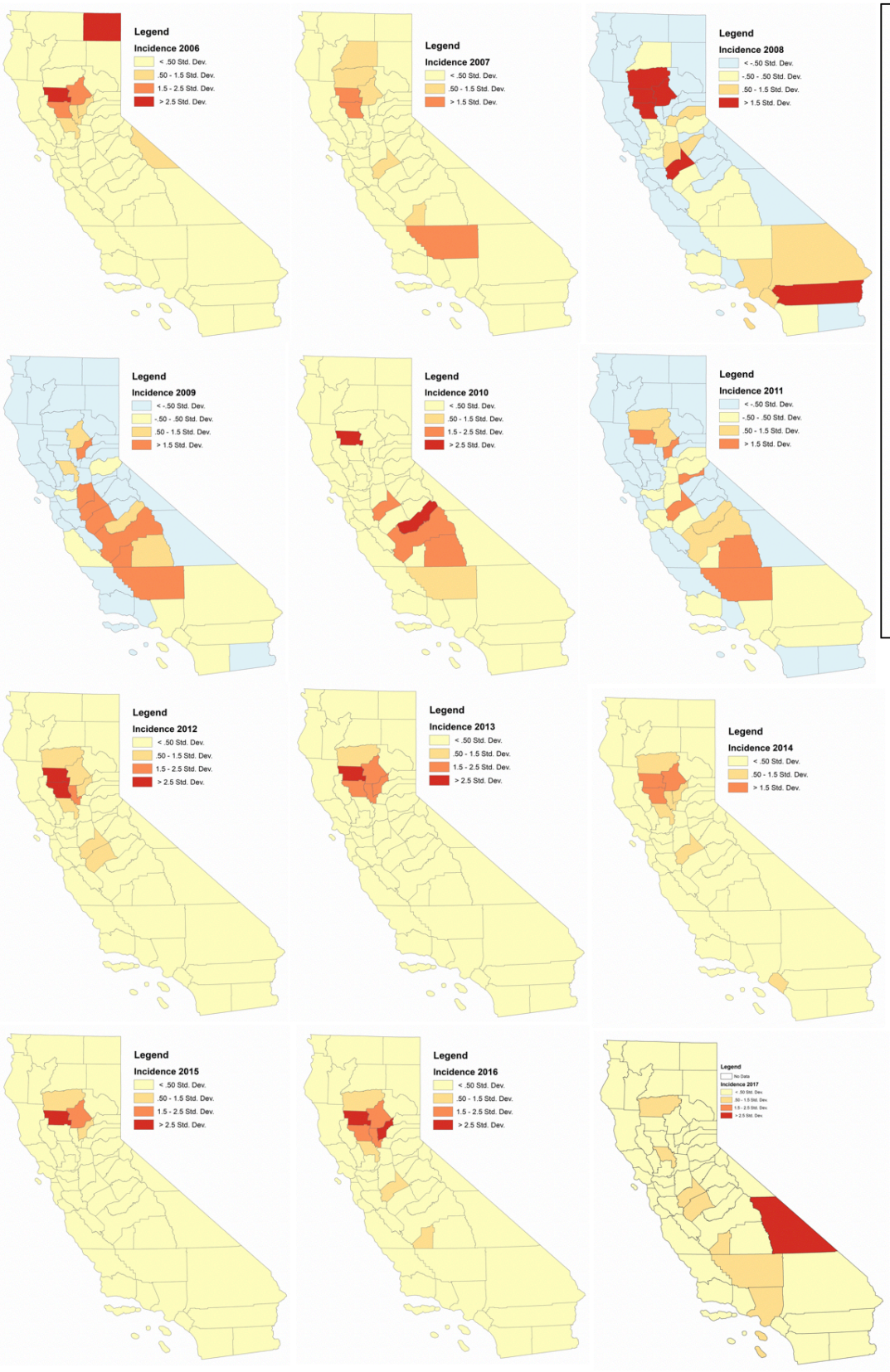

Figure 10: Incidence of human cases for years 2006-2009 (upper row), 2010-2013 (middle row), 2014-2017 (lower row) with color bins based on standard deviations away from the mean. Maps made in ArcMap.

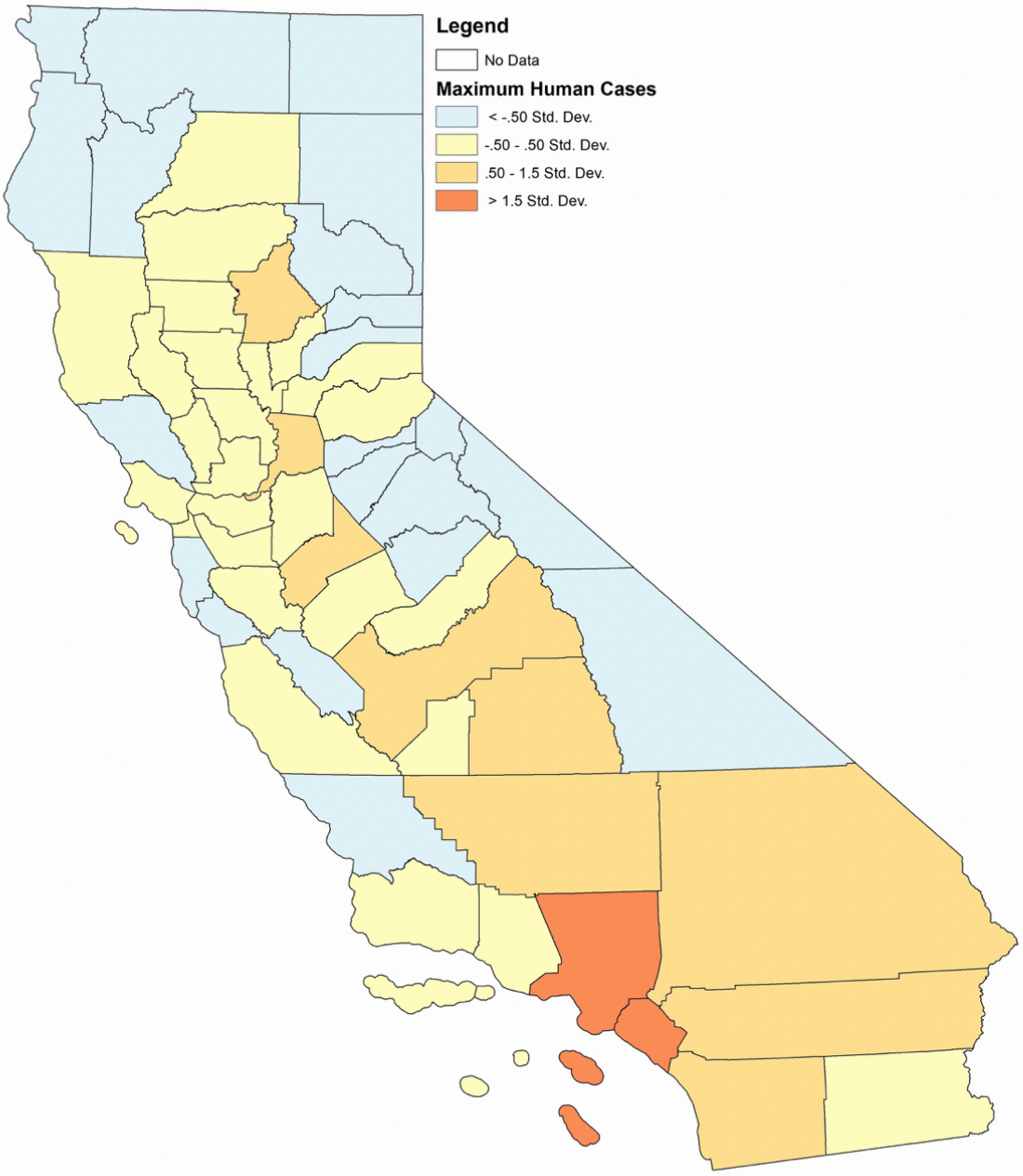

Figure 11: The number of maximum human cases occurring over the span of one week. This was averaged over the years 2006-2017.

8.2 Climate Averages (2006-2017) during Mosquito Incubation Period Maps

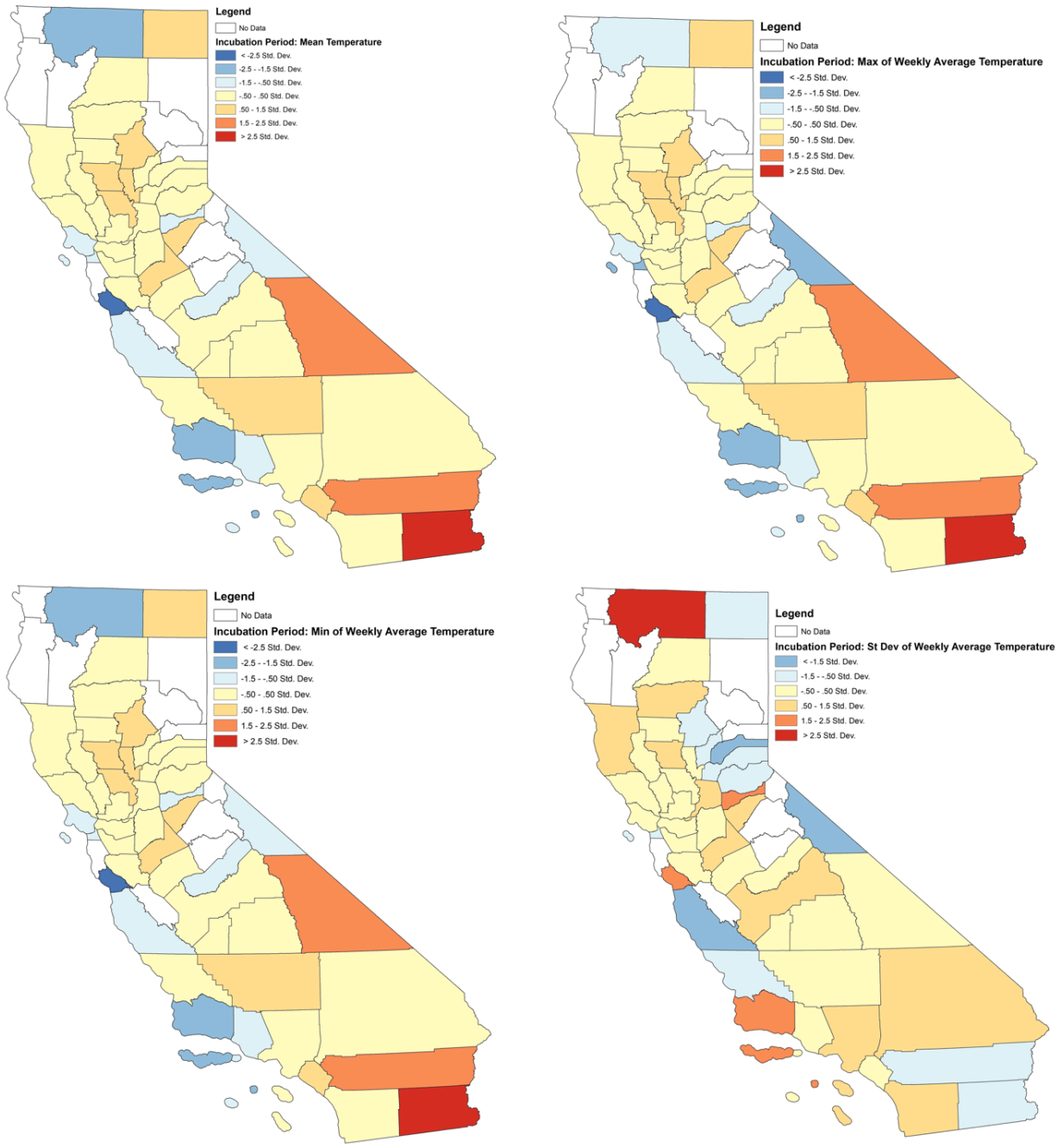

Figure 12: Incubation period mean of temperature (upper left), incubation period maximum of weekly average temperature (upper right), incubation period minimum of weekly average temperature (lower left), and incubation period standard deviation of weekly average temperature (lower right). These incubation period maps were averaged over the years 2006-2017. Temperature is measured in ºC.

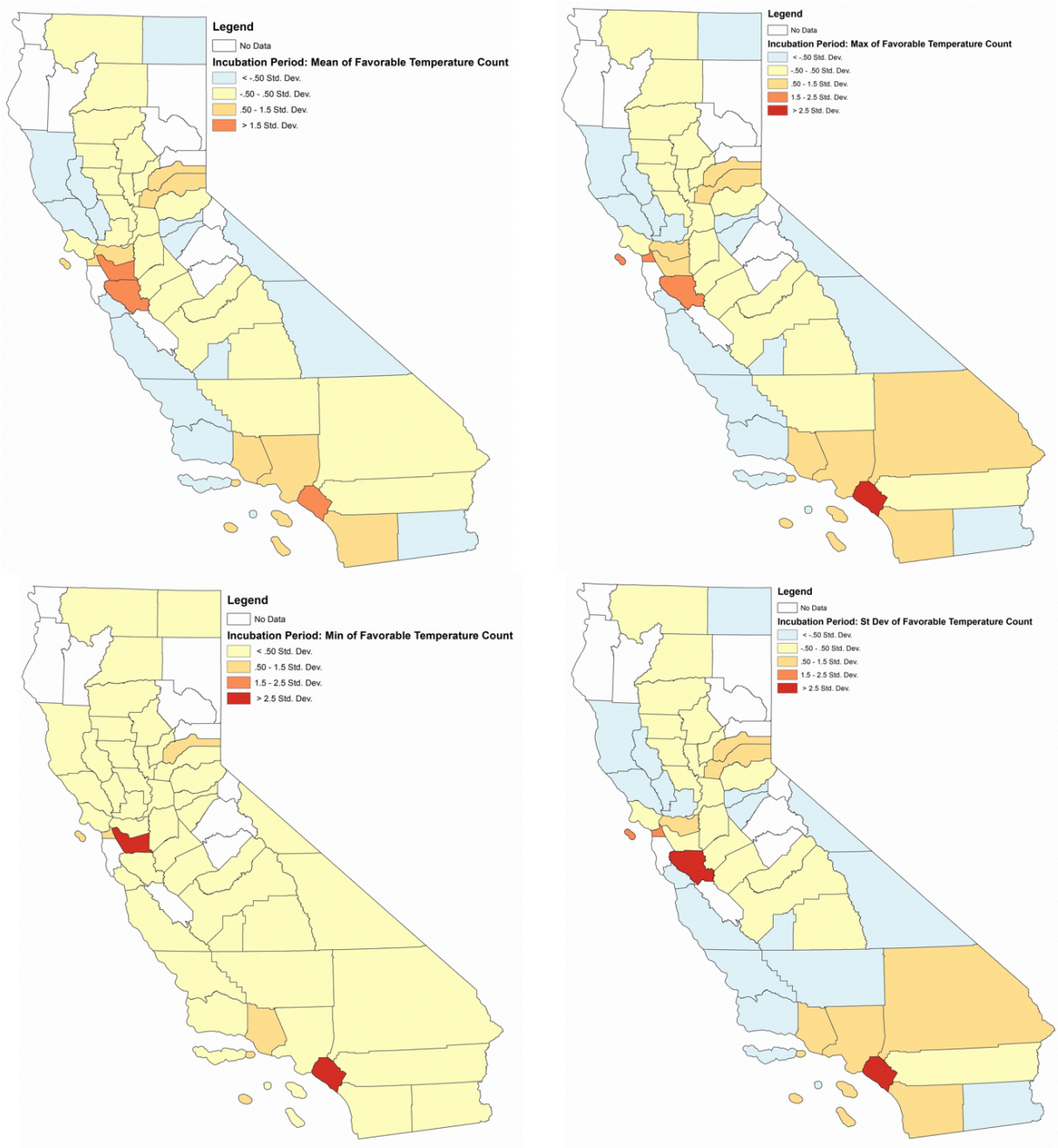

Figure 13: Incubation period mean of favorable temperature count (upper left), incubation period maximum of favorable temperature count (upper right), incubation period minimum of favorable temperature count (lower left), and incubation period standard deviation of favorable temperature count (lower right). These incubation period maps were averaged over the years 2006-2017. This count is measured by the number of days where both the minimum and the maximum daily temperature range is favorable to mosquito activity, which is between 14-30ºC.

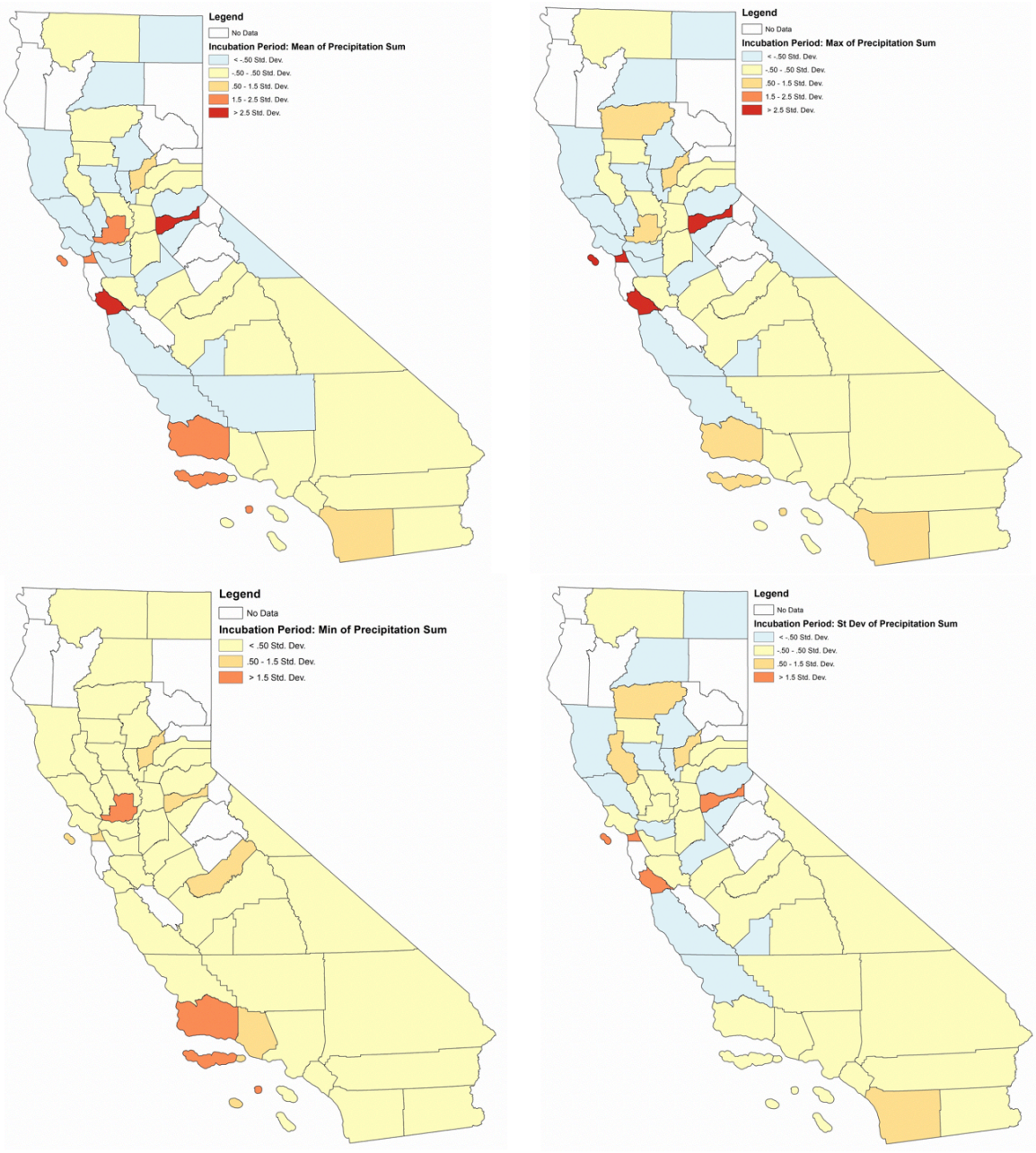

Figure 14: Incubation period mean of precipitation sum (upper left), incubation period maximum precipitation sum (upper right), incubation period minimum of precipitation sum (lower left), and incubation period standard deviation of precipitation sum (lower right). These incubation period maps were averaged over the years 2006-2017. Precipitation sum is measured in millimeters.

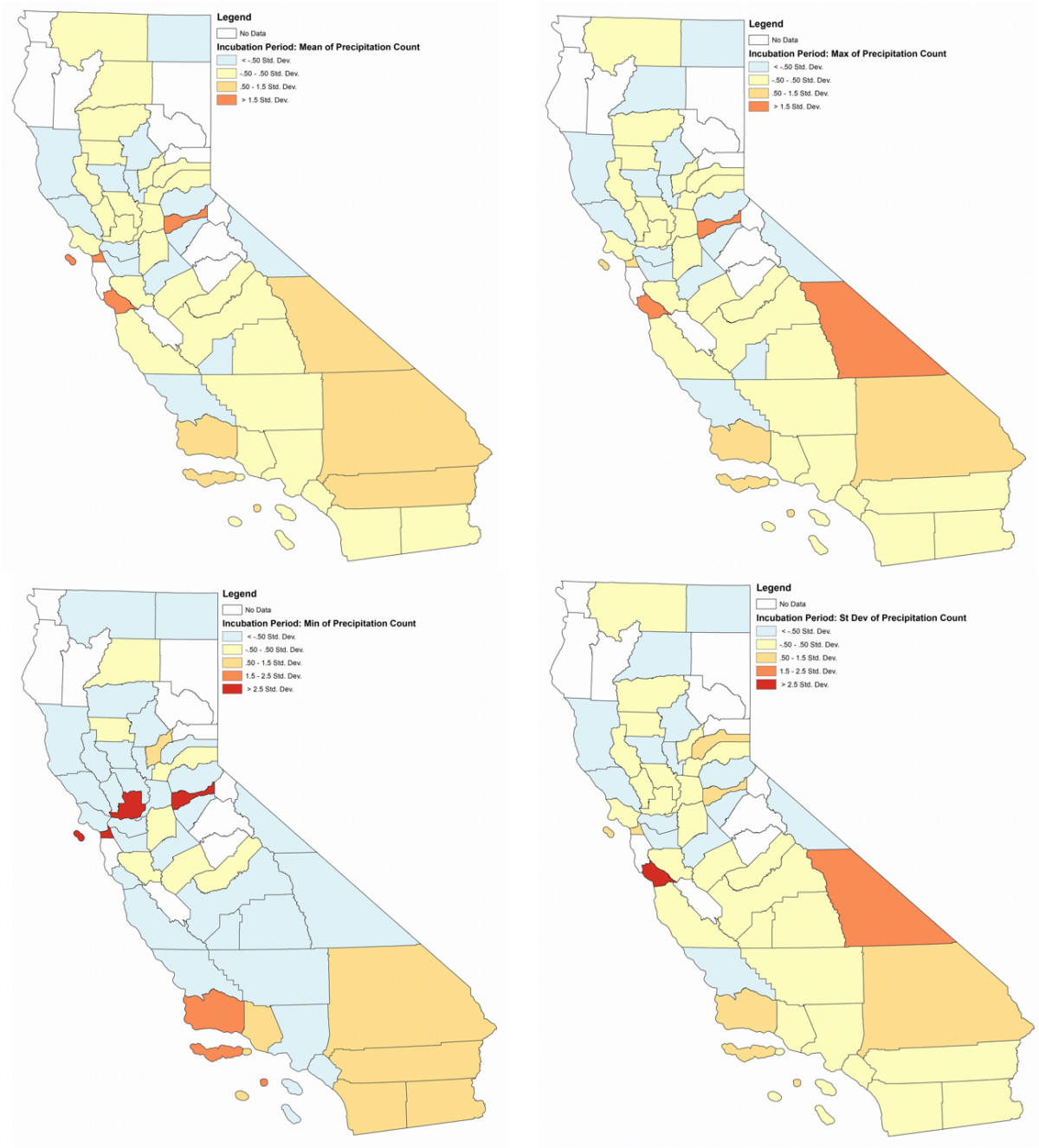

Figure 15: Incubation period mean of precipitation count (upper left), incubation period maximum of precipitation count (upper right), incubation period minimum of precipitation count (lower left), and incubation period standard deviation of precipitation count (lower right). These incubation period maps were averaged over the years 2006-2017. Precipitation count is measured by the number of days with precipitation greater than one millimeter.

8.3 Climate Averages (2006-2017) during Mosquito Lifetime Period Maps

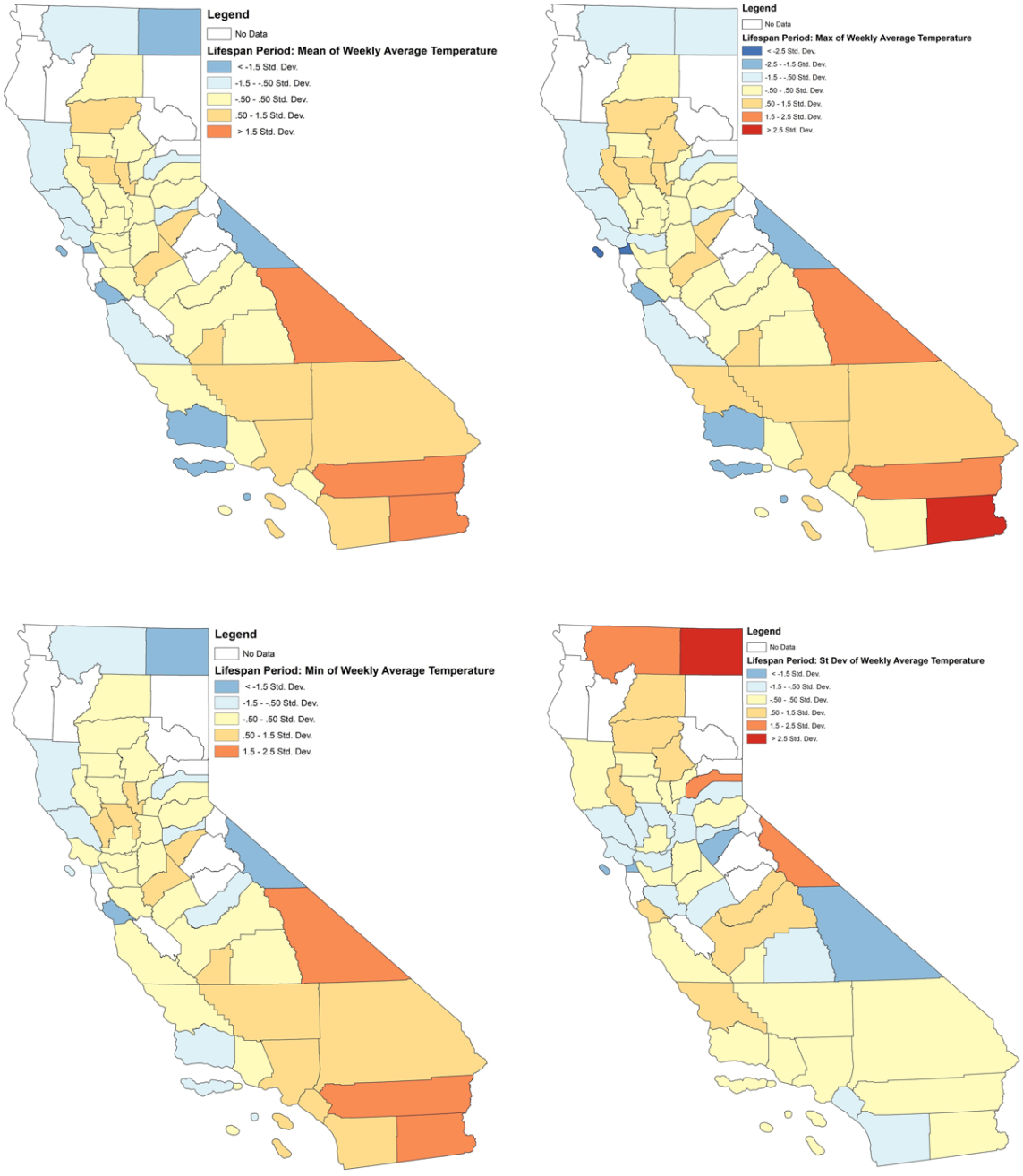

Figure 16: Lifetime period mean of temperature (upper left), lifetime period maximum of weekly average temperature (upper right), lifetime period minimum of weekly average temperature (lower left), and lifetime period standard deviation of weekly average temperature (lower right). These lifetime period maps were averaged over the years 2006-2017. Temperature is measured in ºC.

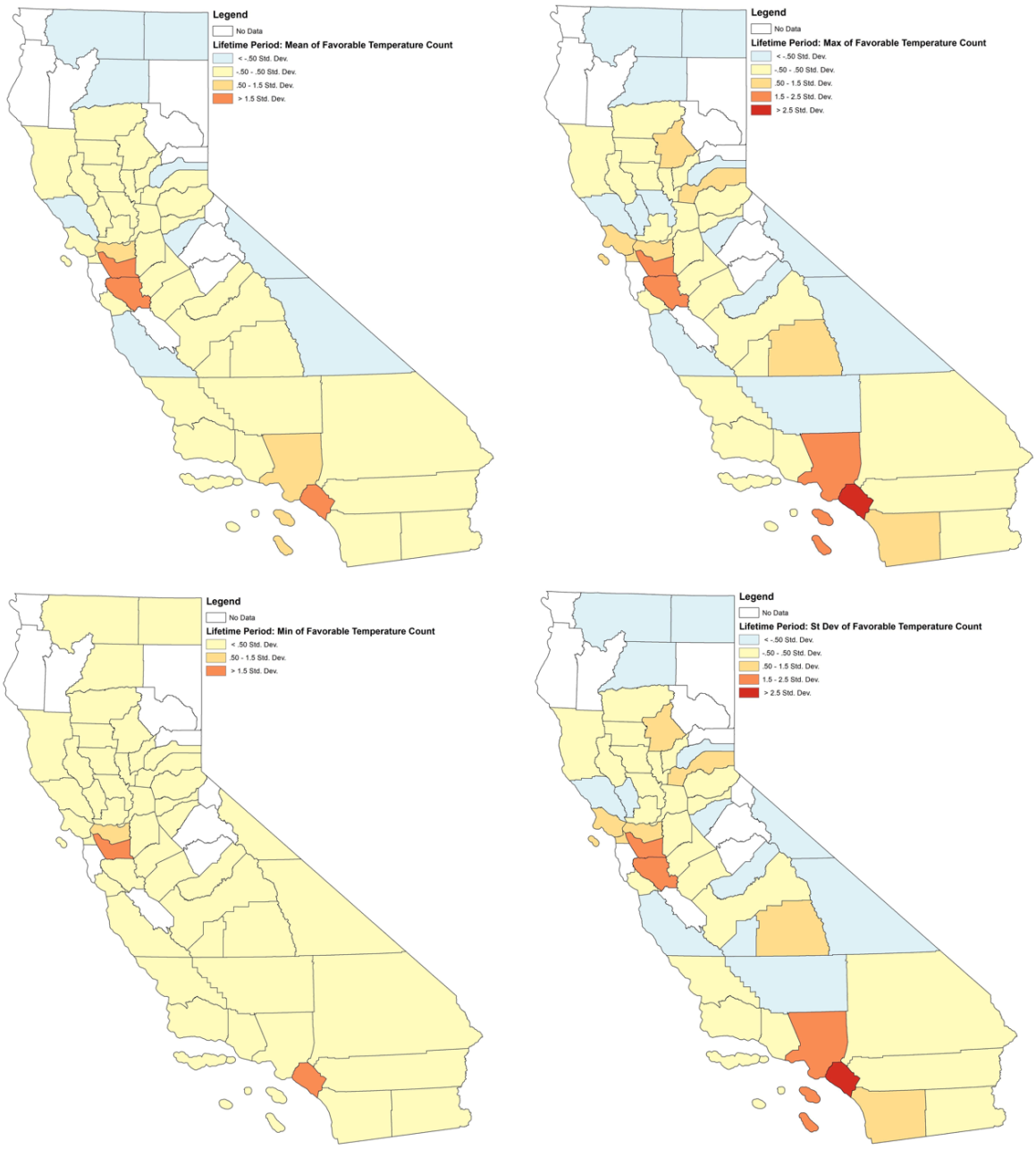

Figure 17: Lifetime period mean of favorable temperature count (upper left), lifetime period maximum of favorable temperature count (upper right), lifetime period minimum of favorable temperature count (lower left), and lifetime period standard deviation of favorable temperature count (lower right). These lifetime period maps were averaged over the years 2006-2017. This count is measured by the number of days where both the minimum and the maximum daily temperature range is favorable to mosquito activity, which is between 14-30ºC.

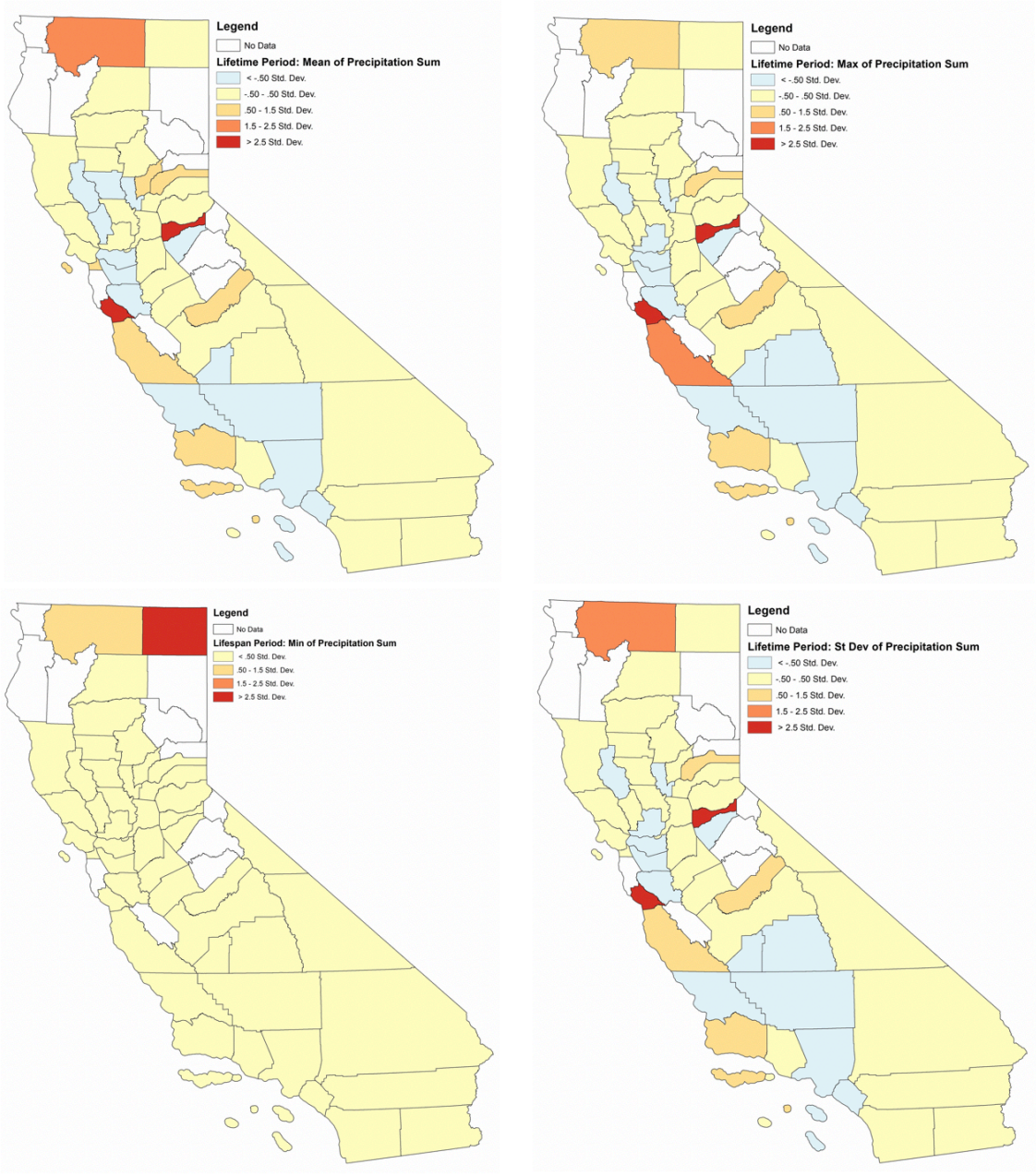

Figure 18: Lifetime period mean of precipitation sum (upper left), lifetime period maximum precipitation sum (upper right), lifetime period minimum of precipitation sum (lower left), and lifetime period standard deviation of precipitation sum (lower right). These lifetime period maps were averaged over the years 2006-2017. Precipitation sum is measured in millimeters.

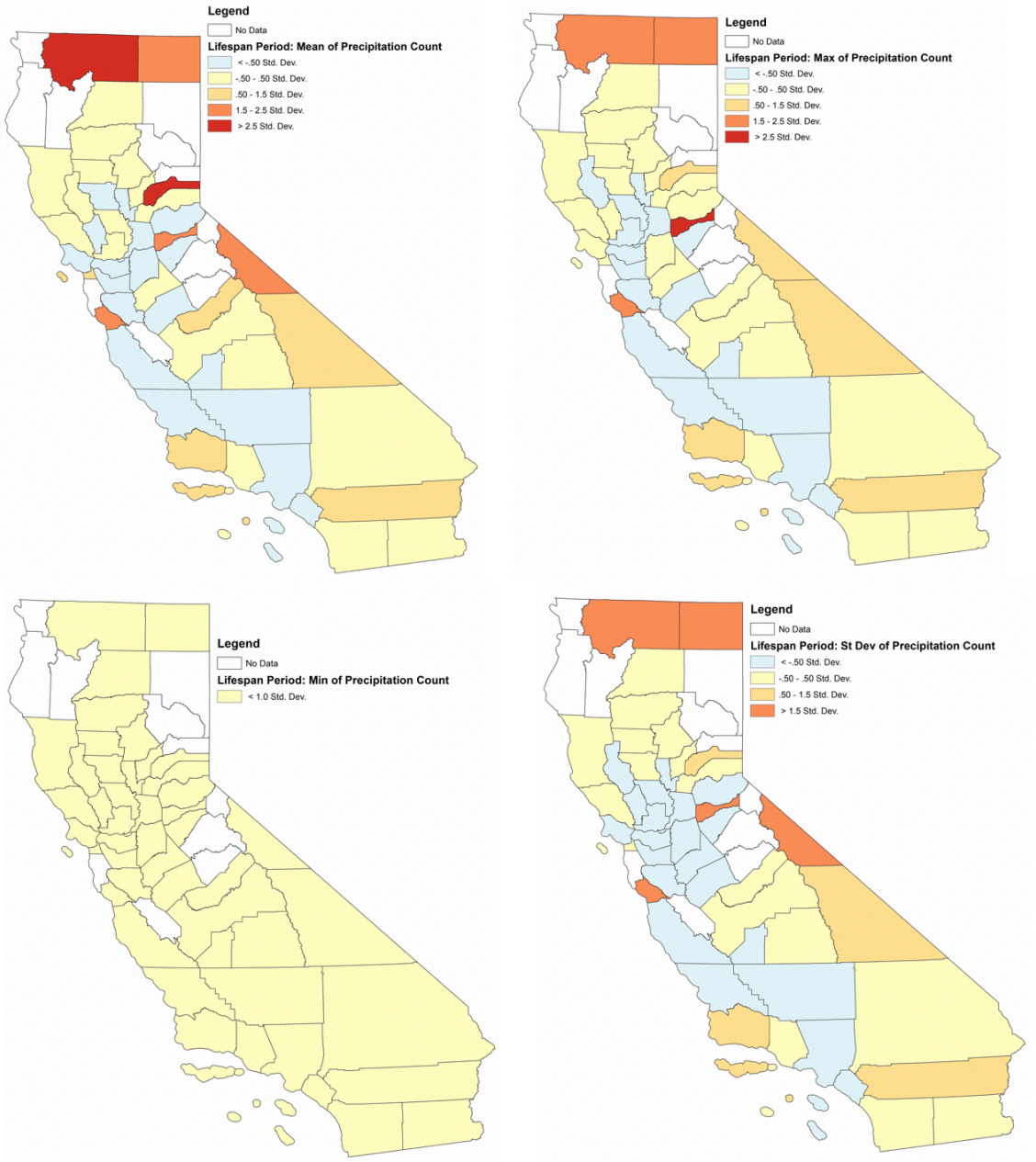

Figure 19: Lifespan period mean of precipitation count (upper left), lifespan period maximum of precipitation count (upper right), lifespan period minimum of precipitation count (lower left), and lifespan period standard deviation of precipitation count (lower right). These lifespan period maps were averaged over the years 2006-2017. Precipitation count is measured by the number of days with precipitation greater than one millimeter.

8.4 Climate Averages (2006-2017) during Mosquito Population Growth Period

Maps

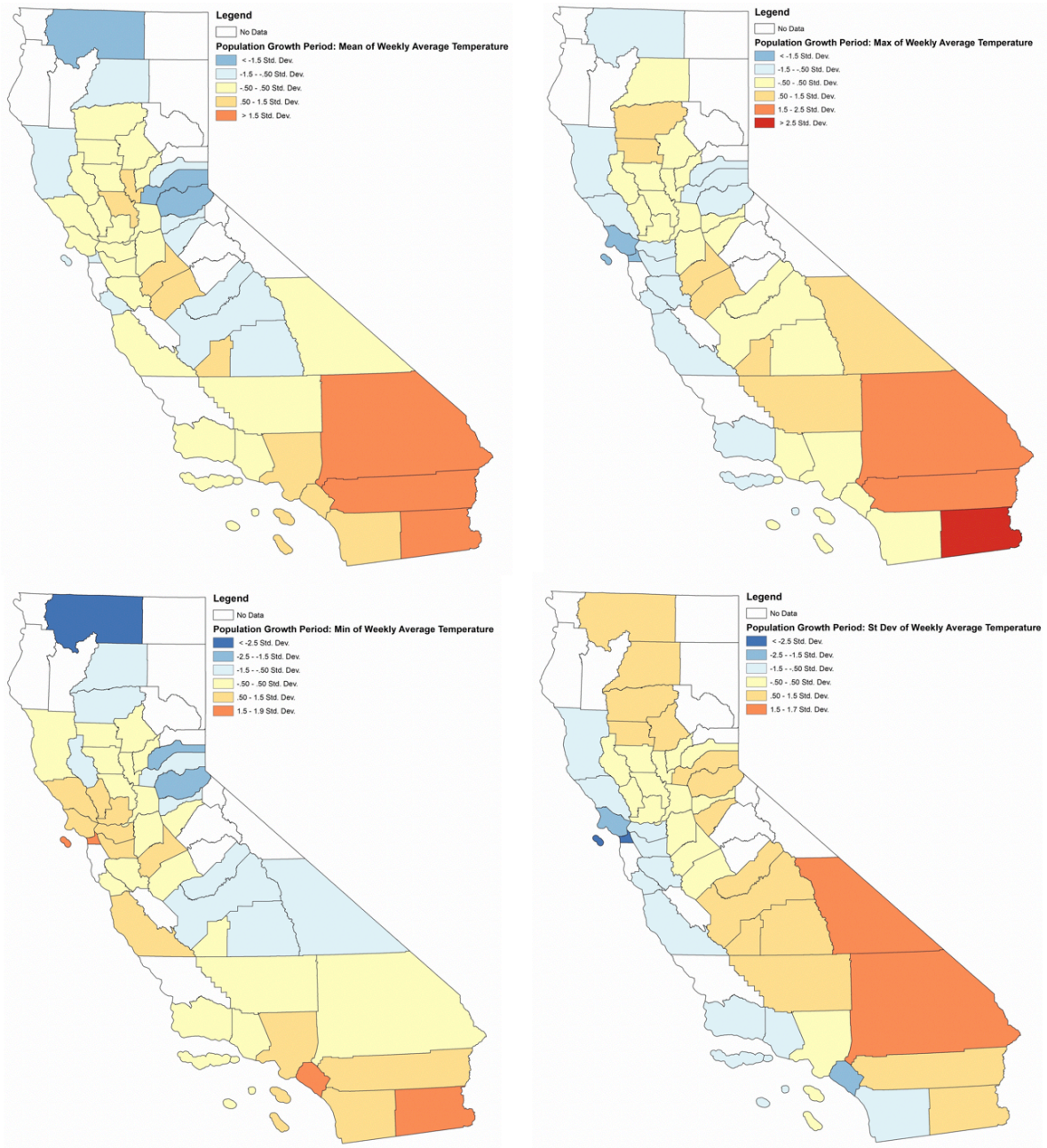

Figure 20: Population growth period mean of temperature (upper left), population growth period maximum of weekly average temperature (upper right), population growth period minimum of weekly average temperature (lower left), and population growth period standard deviation of weekly average temperature (lower right). These population growth period maps were averaged over the years 2006-2017. Temperature is measured in °C.

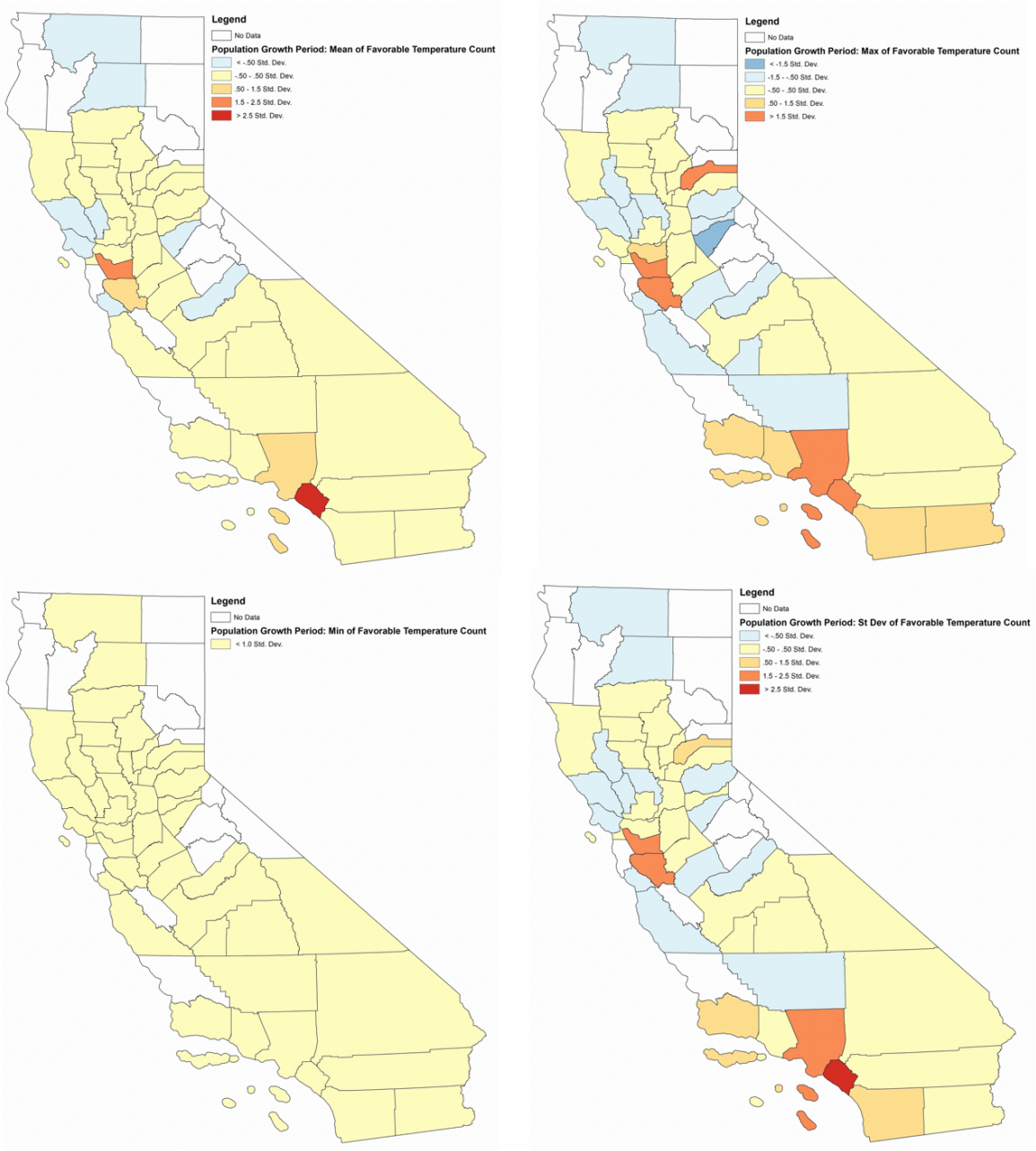

Figure 21: Population growth period mean of favorable temperature count (upper left), population growth period maximum of favorable temperature count (upper right), population growth period minimum of favorable temperature count (lower left), and population growth period standard deviation of favorable temperature count (lower right). These population growth period maps were averaged over the years 2006-2017. This count is measured by the number of days where both the minimum and the maximum daily temperature range is favorable to mosquito activity, which is between 14-30ºC.

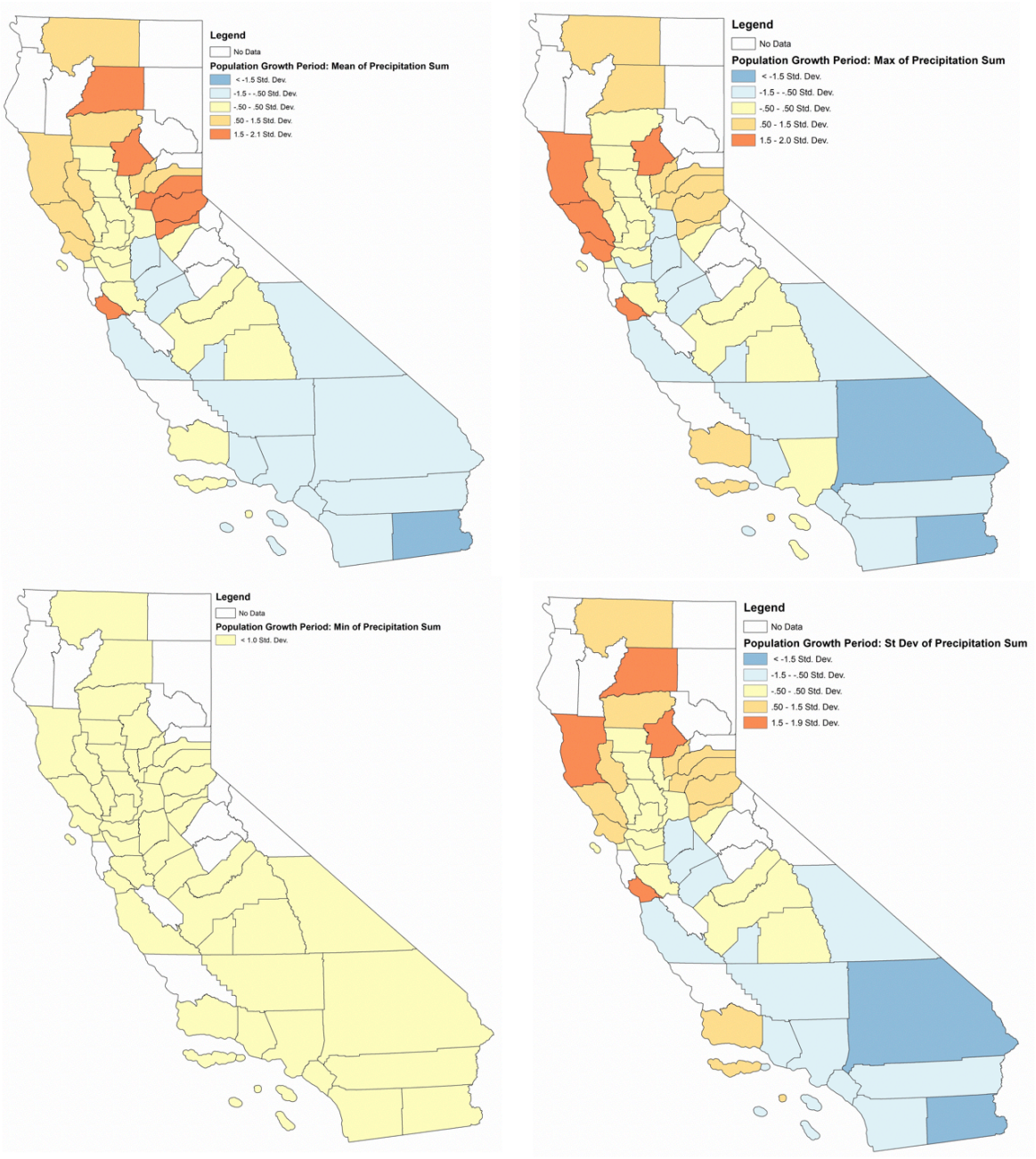

Figure 22: Population growth period mean of precipitation sum (upper left), population growth period maximum precipitation sum (upper right), population growth period minimum of precipitation sum (lower left), and population growth period standard deviation of precipitation sum (lower right). These population growth period maps were averaged over the years 2006-2017. Precipitation sum is measured in millimeters.

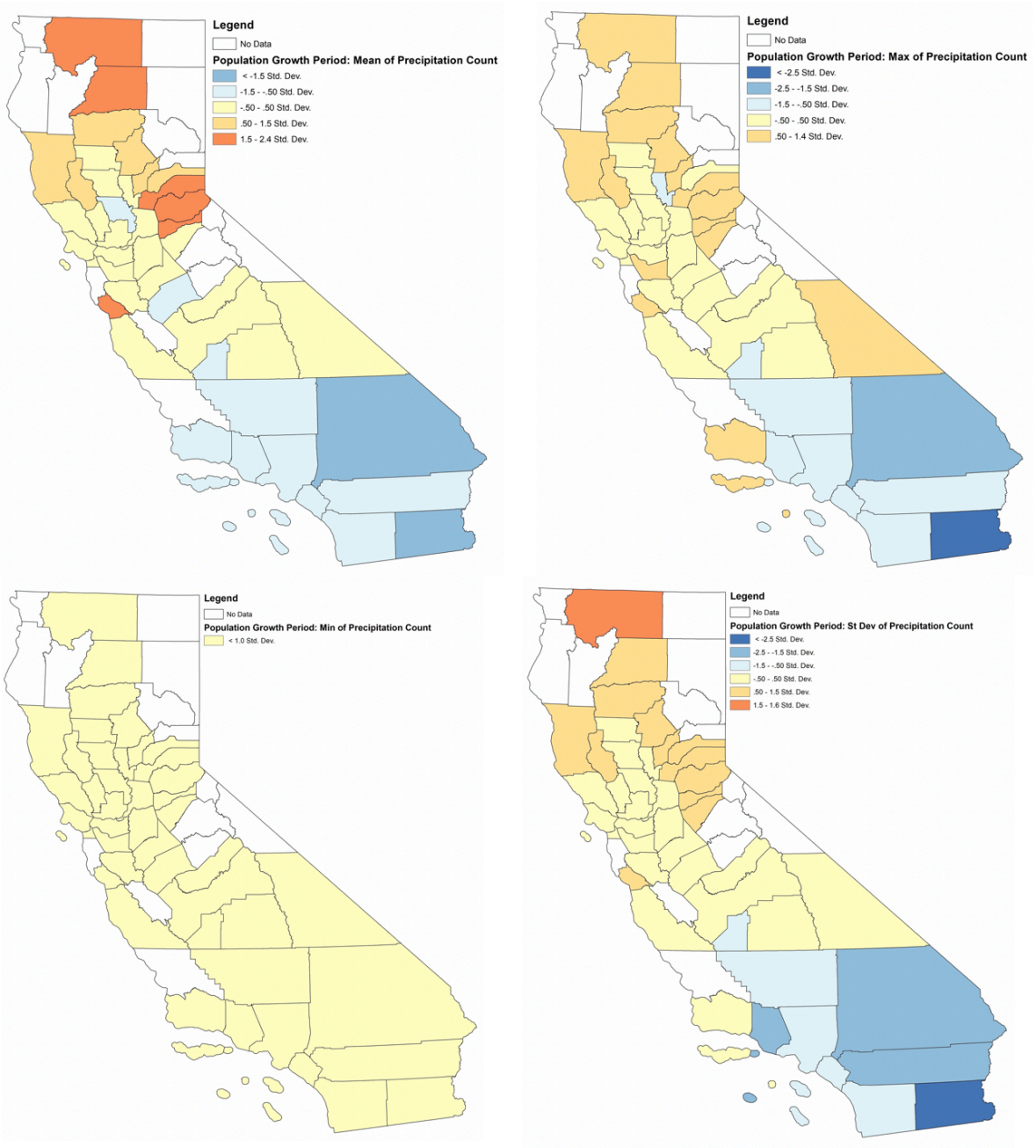

Figure 23: Population growth period mean of precipitation count (upper left), population growth period maximum of precipitation count (upper right), population growth period minimum of precipitation count (lower left), and population growth period standard deviation of precipitation count (lower right). These population growth period maps were averaged over the years 2006-2017. Precipitation count is measured by the number of days with precipitation greater than one millimeter.

8.5 Census Maps

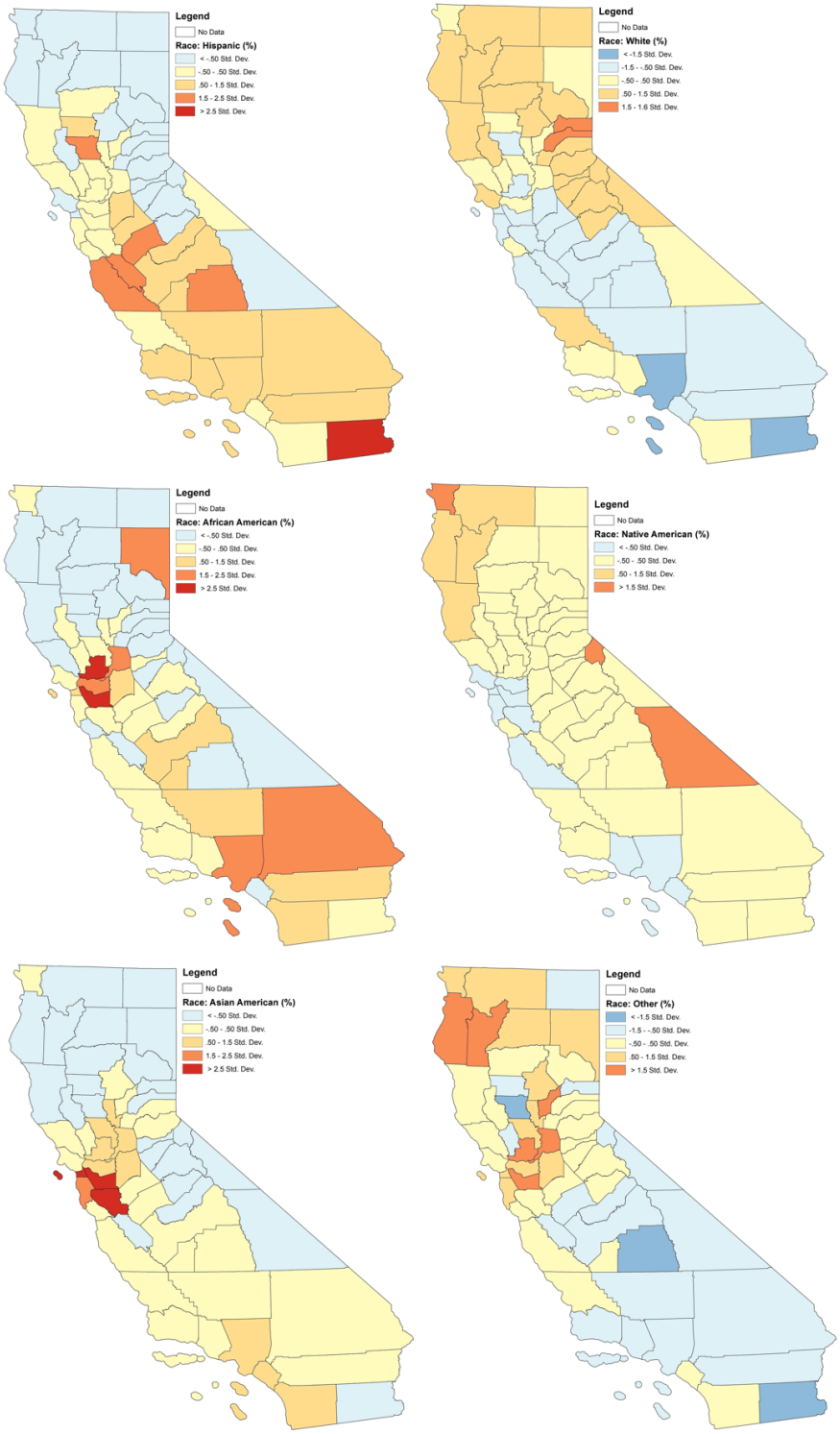

Figure 24:
Race percentages within county populations, with the Hispanic population percentage (upper left), the white population percentage (upper right), the African American population percentage (middle left), the Native American population percentage (middle right), the Asian American population percentage (lower left), and the other population percentage not within these ethnic categories (lower right).

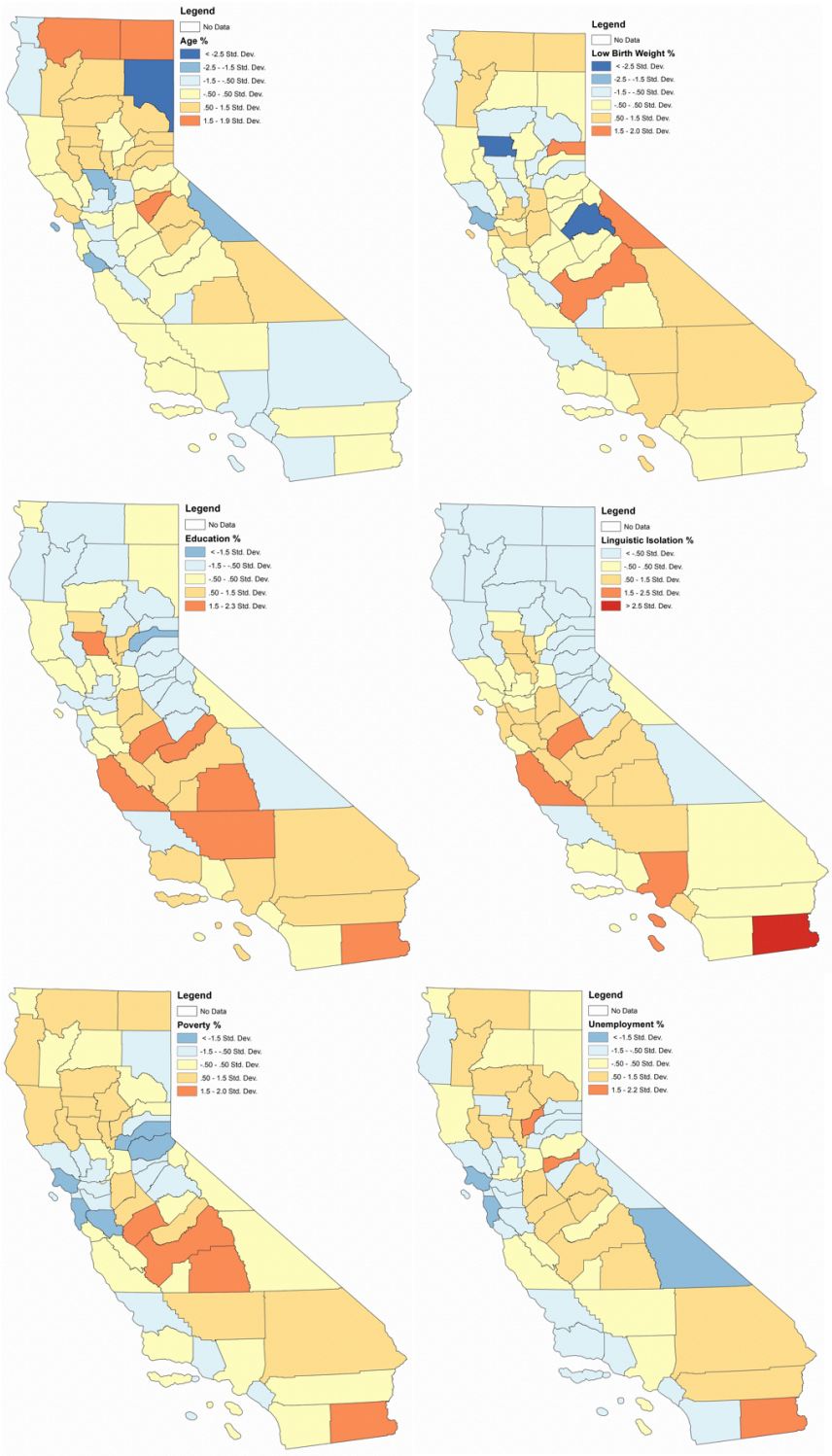

Figure 25: Sociodemographic factor percentages within county populations, with the percent of the population under the age of 10 and over the age of 65 (upper left), the percent of the population with a low birth weight (upper right), the percent of the population over 25 with less than a high school education (middle left), the percent of households in which no one 14 years and over speaks English "very well" or speaks English only (middle right), the percent of the population that is living below two times the federal poverty level (lower left), and the percent of the population over the age of 16 that is unemployed and eligible for the labor force (lower right).

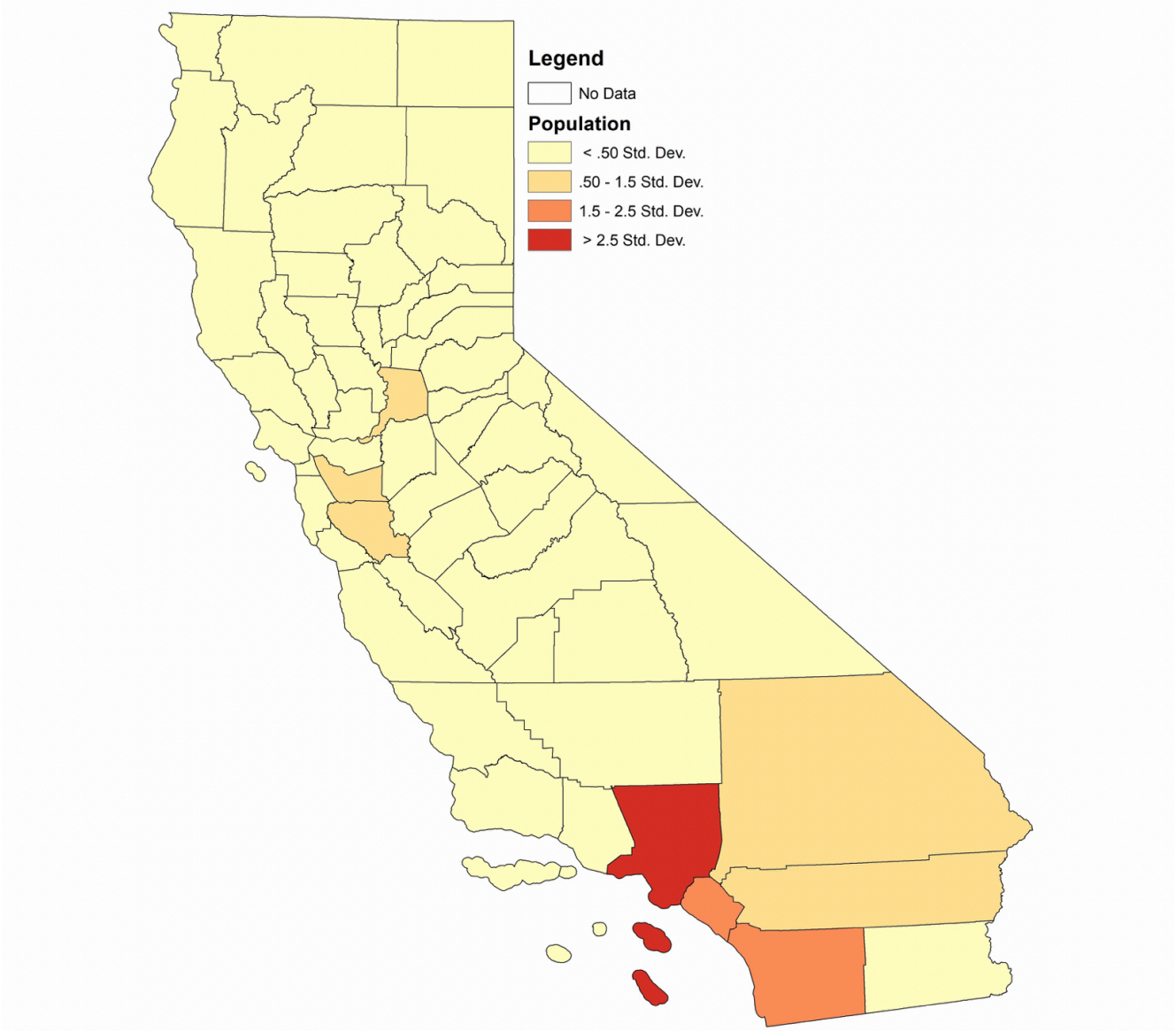

Figure 26: The number of individuals within the county population, averaged over the years 2006-2017 (map made in ArcMap).

8.6 Index Maps

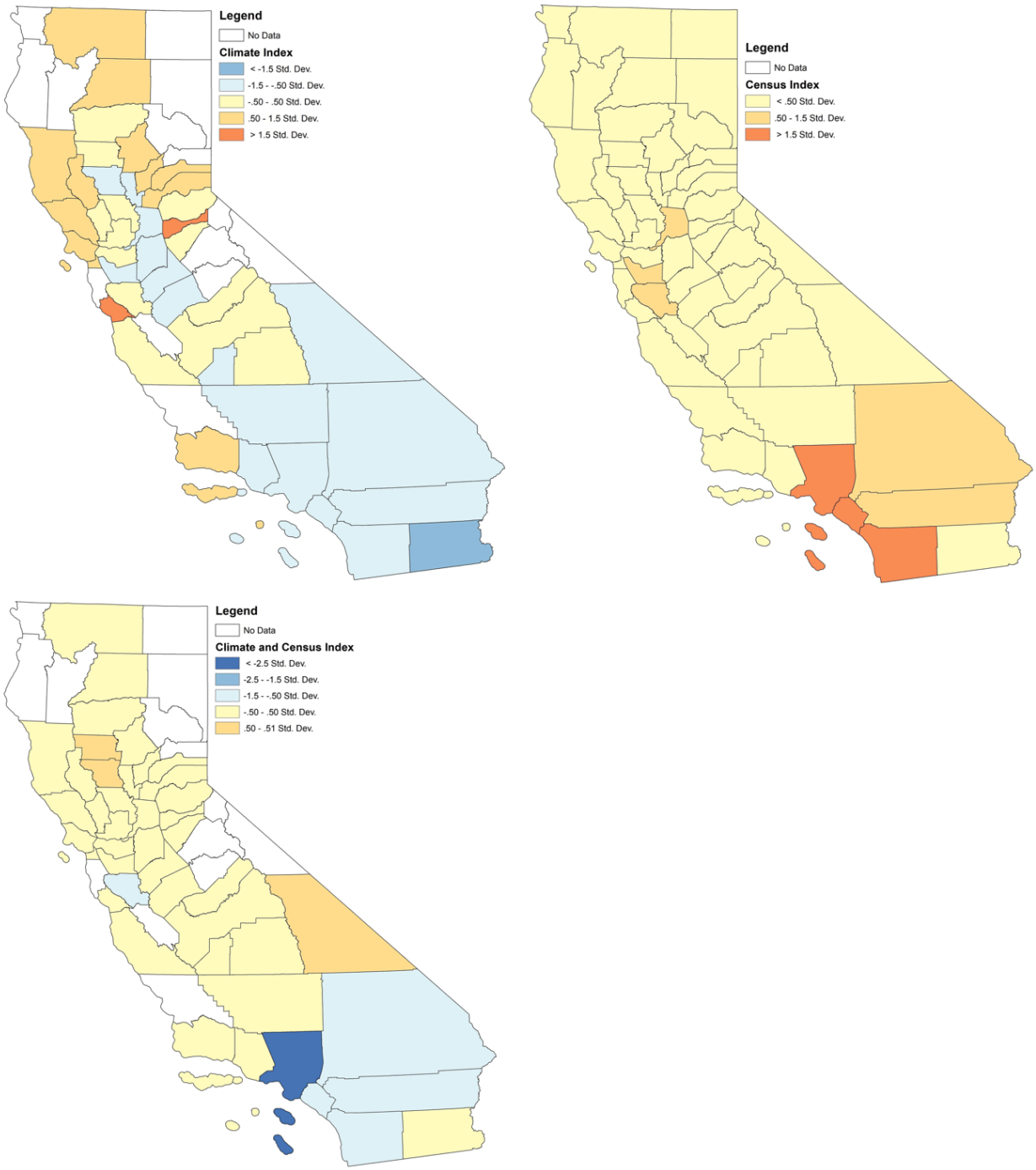

Figure 27: The climate index that takes into account all climate factors from years 2006-2017 (upper left), the census index that takes into account all of the census factors from years 2006-2017 (upper right), and the climate and census index that takes into account all of the climate and census factors from years 2006-2017 (lower left). Maps were made in ArcMap.

8.7 Projection Maps

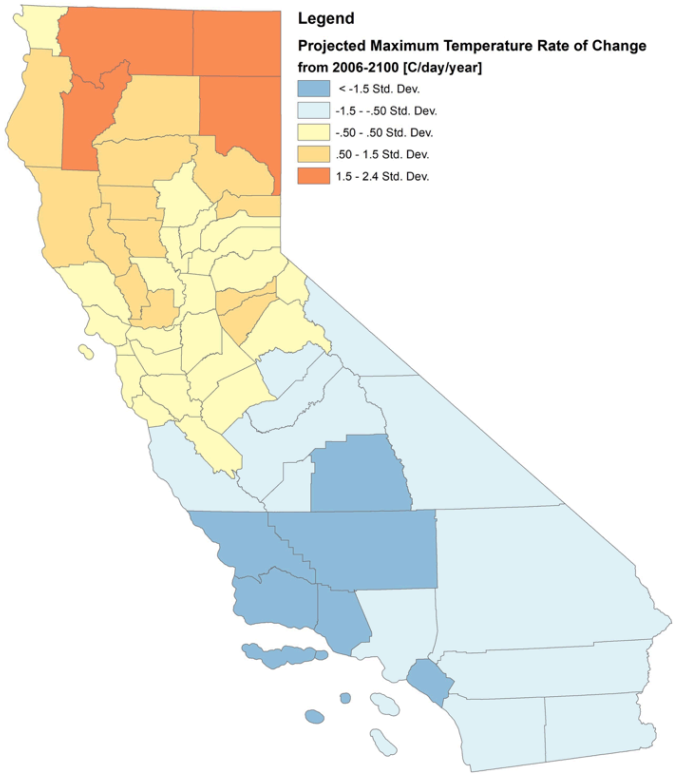

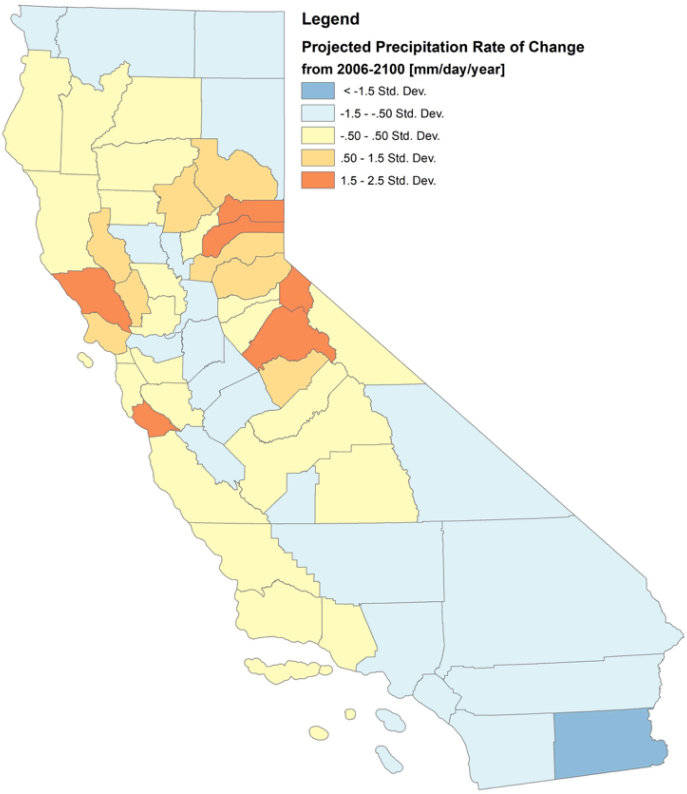

Figure 28: The projected maximum temperature rate of change for the years 2006 to 2100 in ºC/day/year (above) and the projected precipitation rate of change from 2006-2100 in mm/day/year (below). These rates of change were calculated from the Can-ESM2 climate model using the RCP 8.5 projection.

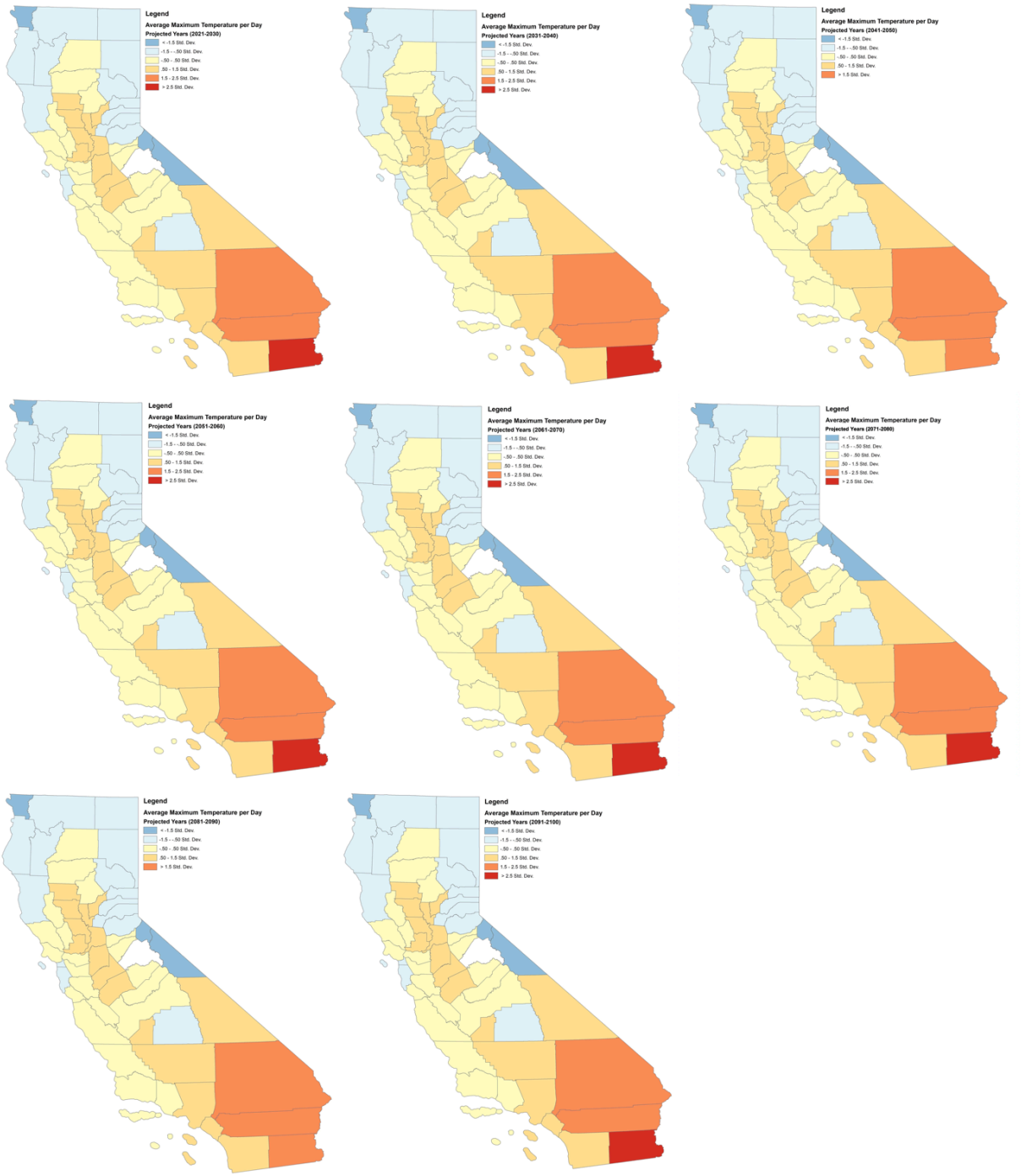

Figure 29: The projected average maximum temperature per day for the decades 2021-2030 (upper left), 2031-2040 (upper middle), 2041-2050 (upper right), 2051-2060 (middle left), 2061-2070 (middle center), 2071-2080 (middle right), 2081-2090 (bottom left), and 2091-2100 (bottom right). These were calculated from the Can-ESM2 climate model using the RCP 8.5 projection.

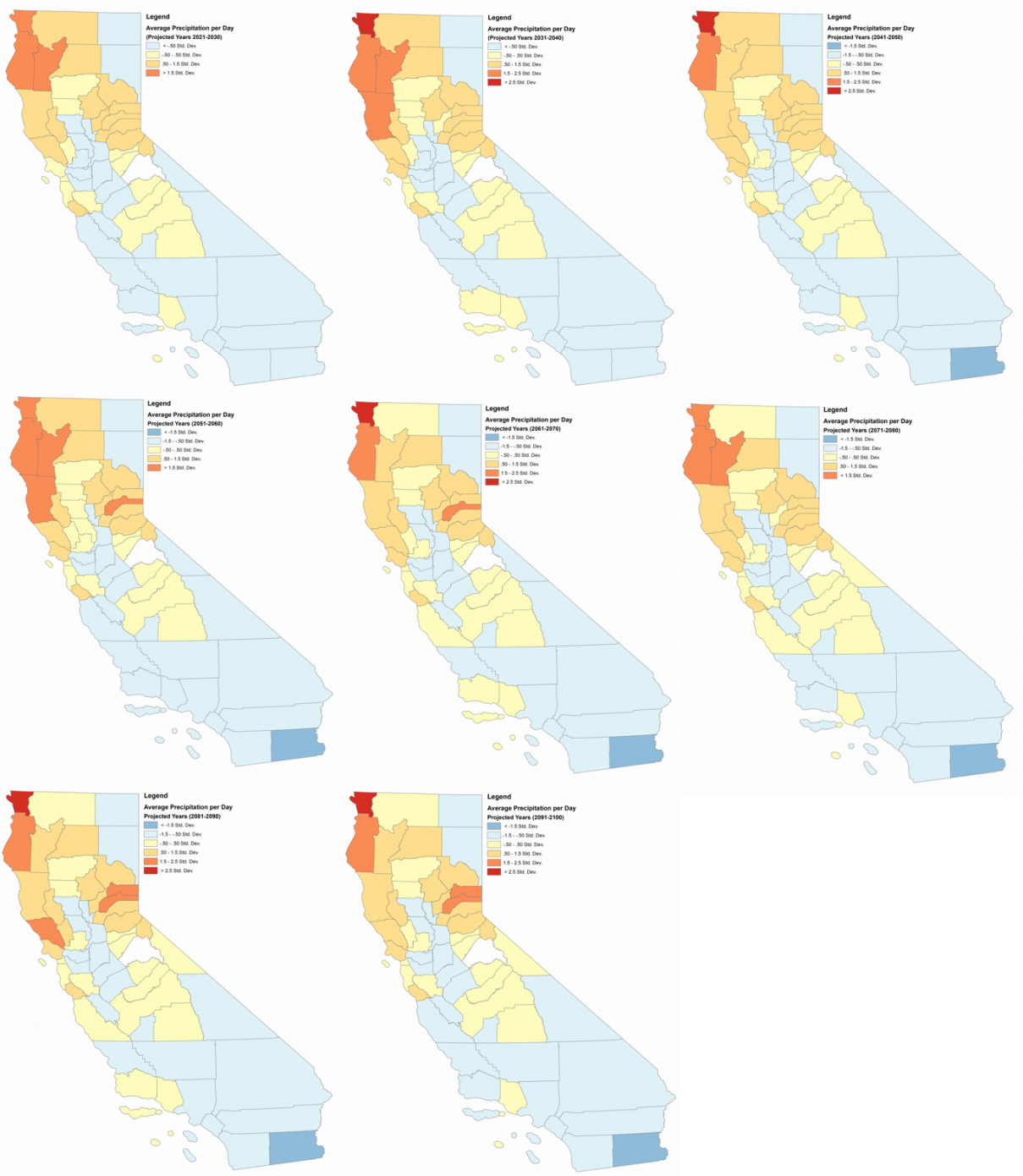

Figure 30: The projected average precipitation per day for the decades 2021-2030 (upper left), 2031-2040 (upper middle), 2041-2050 (upper right), 2051-2060 (middle left), 2061-2070 (middle center), 2071-2080 (middle right), 2081-2090 (bottom left), and 2091-2100 (bottom right). These were calculated from the Can-ESM2 climate model using the RCP 8.5 projection.

8.8 Aspects of the Interactive Vulnerability Map

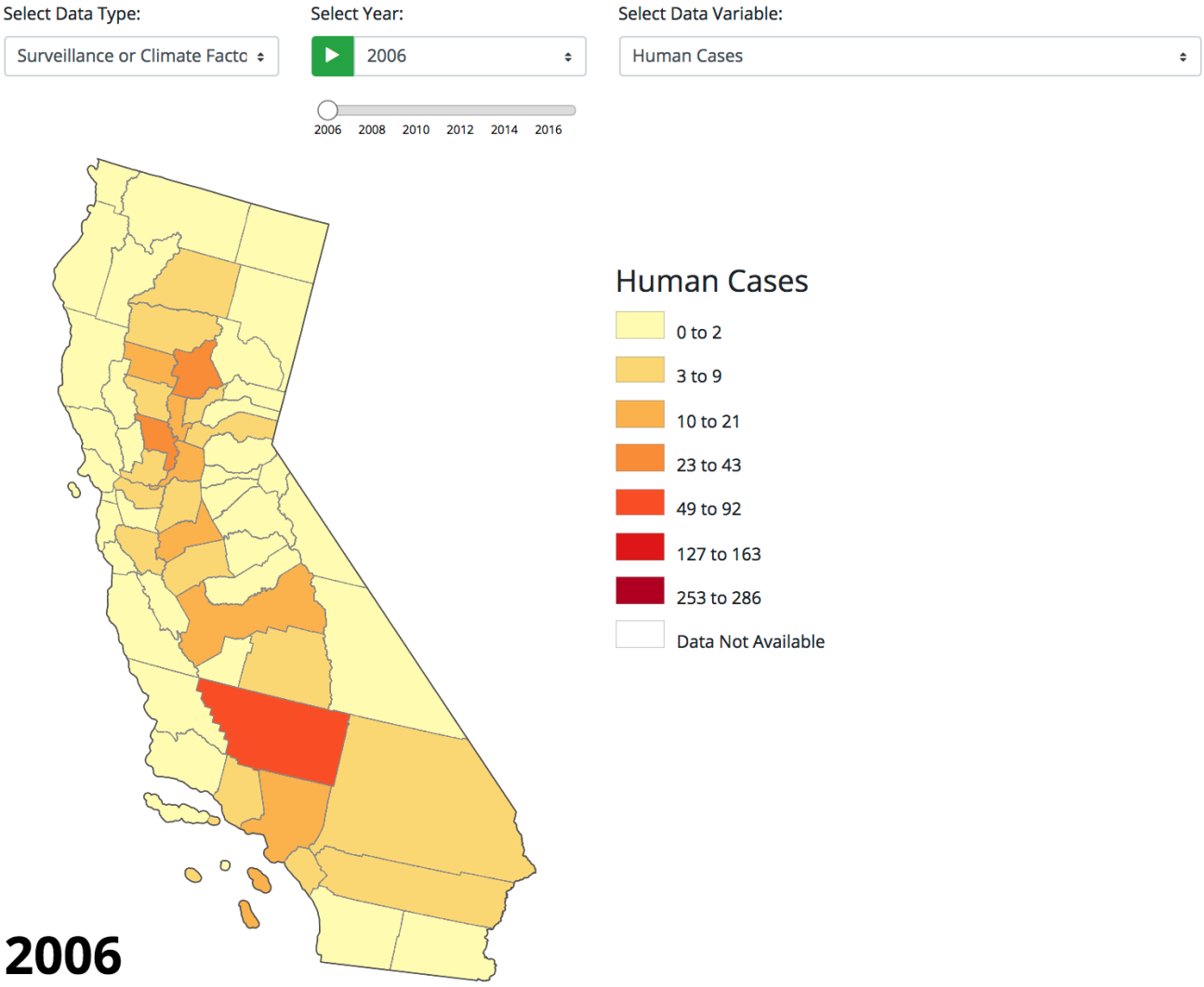

Figure 31: A view of the interactive vulnerability map webpage. In this image, the human cases for the year 2006 was selected to view. The data type, the year, and the data variable can be selected. Furthermore, the time period can be animated.

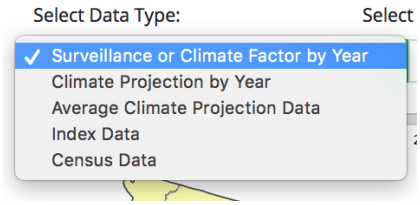

a.

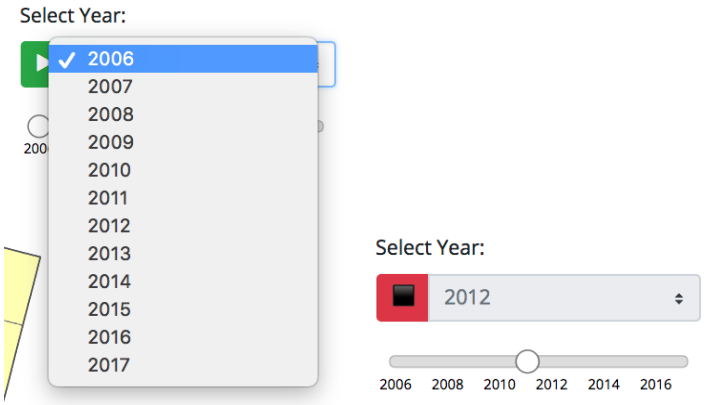

b.

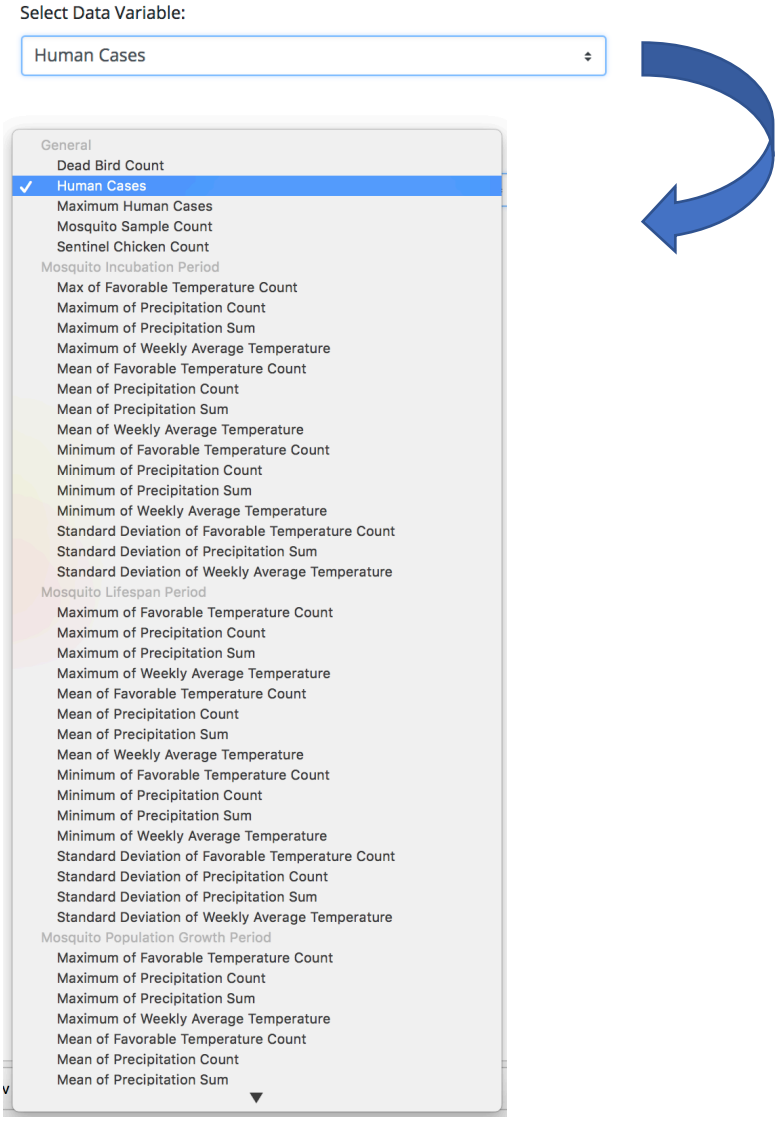

c.

Figure 32: Detailed view of the various features that can be selected.
The data type can be selected from a drop-down menu, which are categorized as surveillance or climate factor by year, climate projection by year, average climate projection data, index data, and census data (a).
The year for the given data type can be selected from a drop-down menu, and an automated playthrough animation of the time period can be selected for the given variable (b).
The data variable can be selected from a drop-down menu based on which data type was previously chosen (c).

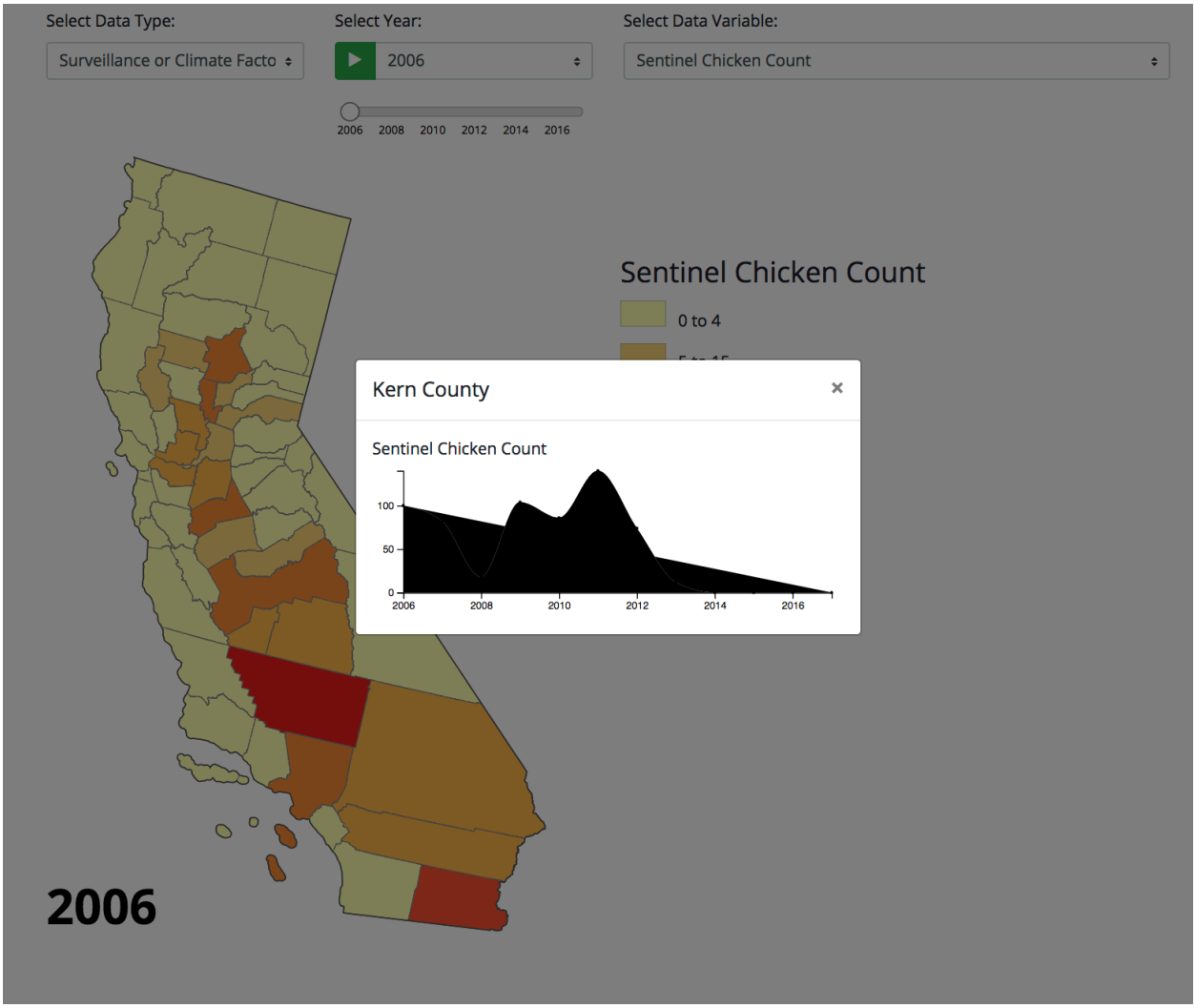

Figure 33: A view of the interactive vulnerability map's pop-up feature. When a data variable with a relevant time period is selected, a desired county may be clicked directly on the California map, and a pop-up plot of the selected variable over time for the given county appears. In this example, the selected variable is Sentinel Chicken Count, and Kern county has been clicked upon the colored map.